Generation of EBV-transformed cell lines

EBV-transformed cell lines (EBV-LCLs) were generated by in vitro transformation of human B cells with EBV (strain B95-8), as described elsewhere (10). Based on the results of *STAT1* sequence analysis, EBV-LCLs from Patient 1 with T385M and wild-type (Wt) alleles and Patient 3 with R274Q and Wt alleles were designated as T385M/Wt and R274Q/Wt, respectively. Two age-matched control EBV-LCLs, designated Wt-1 and Wt-2, were used as controls. EBV-LCLs from Patient 2 were not obtained.

Stimulation reagents

For stimulation, 1:1000 diluted recombinant human IFN-γ 1a (Shionogi, Osaka, Japan; 1000 JRU/ml, 200 ng/ml), 1500 U/ml recombinant human IFN-α (Biosource International, Camarillo, CA), 20 ng/ml IL-27 (R&D Systems, Minneapolis, MN), and 100 μg/ml Curdlan (Wako, Osaka, Japan) were used.

DNA isolation, PCR, and sequence analysis of PCR products and TOPO-TA clones

These procedures were performed following the methods described elsewhere (10).

Measurement of CXCL10 (IP-10) concentration in supernatant of monocyte-derived macrophages and EBV-LCLs using Cytometric Bead Array

To accurately evaluate STAT1 function by studying supernatant IP-10 production from macrophages, monocytes were first purified from PBMCs with CD14 MicroBeads (Miltenyi Biotec, Bergisch Gladbach, Germany) to avoid contamination of other cells. A total of 5×10^5 cells/ml monocytes was then differentiated into macrophages by culturing for 7 d in RPMI 1640 containing 10% FBS in the presence of 5 ng/ml M-CSF (R&D Systems). To determine the effect of IFN-γ, differentiated macrophages in triplicate were not stimulated, were stimulated with 1 μg/ml LPS (Sigma, St Louis, MO), or were prestimulated with 1000 U/ml (200 ng/ml) IFN-γ (Shionogi) for 2 h and then stimulated with 1 μg/ml LPS for 24 h (IFN-γ–LPS stimulation), and supernatant was harvested for IP-10 measurement. For studying IP-10 production from EBV-LCLs, 1×10^6 cells/ml EBV-LCLs were cultured in the presence of 1000 U/ml IFN-γ for 6 h. The concentration of IP-10 in the supernatant was measured with Cytometric Bead Array (BD, San Diego, CA), following the manufacturer's instructions. Data from triplicate independent experiments are reported as the mean ± SD.

Preparation of nuclear extract

Nuclear extract was prepared essentially as described previously (11). Briefly, harvested cells were washed with Ca^{2+} and Mg^{2+}-free PBS and pelleted by centrifugation at 1500 × *g* for 5 min at 4°C. The resulting cell pellets were resuspended in cytoplasmic extract buffer (10 mM HEPES [pH 7.9], 10 mM KCl, 0.1 mM EDTA, 0.1 mM EGTA, 1 mM DTT, 1 mM Na_3VO_4, 1 mM NaF [pH 8]) with the addition of the recommended volume of dissolved protease inhibitor mixture tablets (Roche). After incubation on ice for 15 min, a 1:16 volume of 10% Nonidet P-40 was added. The suspension was vortexed and then centrifuged at 1500 × *g* for 5 min at 4°C. The pellets were washed again with cytoplasmic extract buffer without Nonidet P-40, resuspended with nuclear extract buffer (20 mM HEPES [pH 7.9], 400 mM NaCl, 1 mM EDTA, 1 mM EGTA, 1 mM DTT, 1 mM Na_3VO_4, 1 mM NaF [pH 8]) with the addition of protease inhibitor, and incubated at 4°C for 30 min. After centrifugation at maximum speed for 5 min at 4°C, the supernatant was saved as nuclear extract. Protein concentration was measured by Protein Assay (Bio-Rad, Hercules, CA).

Western blot analysis

After addition of SDS sample buffer, 10 μg nuclear extract was separated by 7.5% polyacrylamide gels and transferred to Immobilon-P Transfer Membranes (Millipore, Billerica, MA). Anti-lamin A Ab (BioLegend, San Diego, CA) was used as a loading control for nuclear extract. All of the primary Abs were used at the final concentration of 1 μg/ml. HRP-conjugated anti-mouse IgG secondary Abs (GE Healthcare, Buckinghamshire, U.K.) were used at 1:2000 dilution. The blots were then visualized by Pierce Western blotting Substrate (Thermo, Rockford, IL).

Studies of STAT1 phosphorylation state and staurosporine and pervanadate treatment of cells

We assessed dephosphorylation with the tyrosine kinase inhibitor staurosporine in EBV-LCLs. A total of 1×10^6 cells/ml EBV-LCLs was stimulated with IFN-γ for 30 min and then incubated with 1 μM staurosporine (Alomone Labs, Jerusalem, Israel) for 15, 30, or 60 min. The phosphatase inhibitor pervanadate was prepared by mixing 200 mM sodium orthovanadate (Wako, Osaka, Japan) and 100 mM H_2O_2 at a 2:1 ratio for 15 min at 22°C. EBV-LCLs were treated with pervanadate (0.8 mM orthovanadate and 0.2 mM H_2O_2) for 5 min and then stimulated with IFN-γ for 30 min. The nuclear extract from each condition was subjected to SDS-PAGE. The phosphorylation state of STAT1 was evaluated with anti-human STAT1 (pY701) Ab purchased from BD. The membrane was then stripped and reprobed with anti-human STAT1 (BD) and anti-lamin A (BioLegend) Abs.

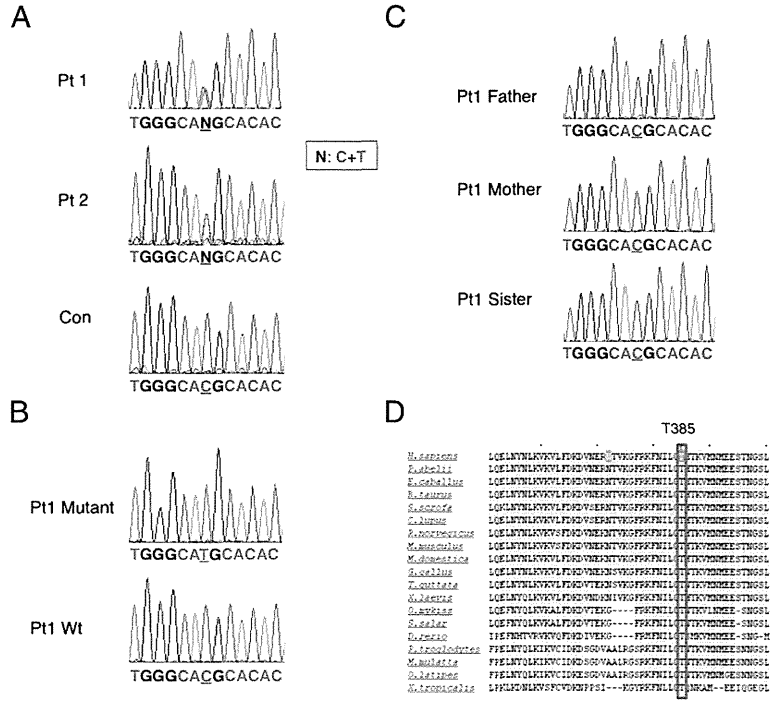

FIGURE 1. Patients 1 and 2 had the same heterozygous base change of c.1153C>T resulting in p.T385M in *STAT1*. (**A**) Direct sequence analysis of *STAT1* exon 14 in Patient 1 (Pt1) and Patient 2 (Pt2). Forward sequence is shown. (**B**) Sequence analysis of TOPO-TA clones of *STAT1* exon 14 PCR products in Patient 1. Mutant and Wt sequences are shown. (**C**) Direct sequence analysis of *STAT1* exon 14 in Patient 1's family members. (**D**) Comparison of the amino acid sequences of STAT1 in different species. The red box indicates the amino acids corresponding to p.T385 in humans. Con, Control.

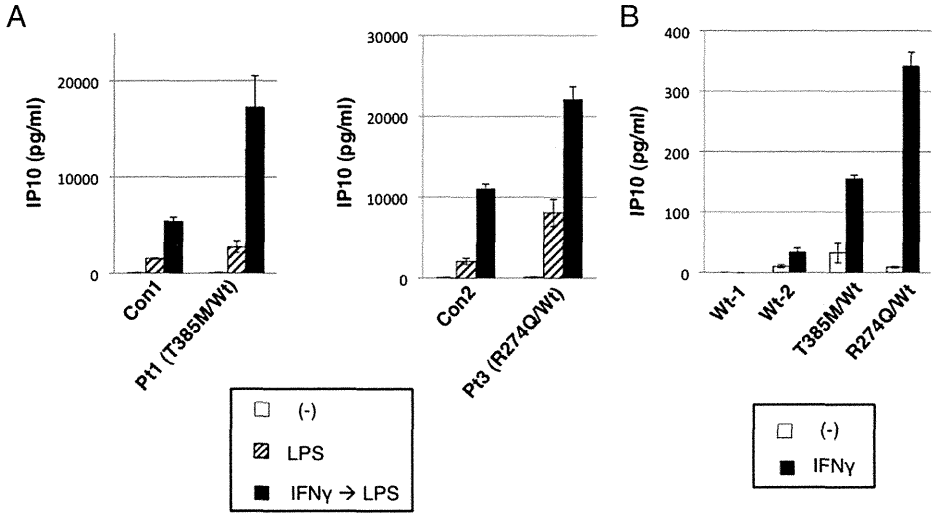

FIGURE 2. T385M was associated with higher levels of IP-10 production following IFN-γ stimulation in monocyte-derived macrophages and in EBV-LCLs. (**A**) Monocyte-derived macrophages were cultured in the presence of media, LPS, or IFN-γ–LPS for 24 h. IP-10 production was studied in the supernatant. Data shown are mean ± SD of triplicate independent experiments. (**B**) EBV-LCLs were stimulated with IFN-γ for 6 h, and IP-10 production was studied in the supernatant. Data shown are mean ± SD of triplicate independent experiments. Con1, Control for Patient 1 obtained and analyzed at the same time; Con2, control for Patient 3 obtained and analyzed at the same time; Pt1, Patient 1; Pt3, Patient 3; (−), media.

Flow cytometric analysis of intracellular IL-17A expression in CD4$^+$ cells

PBMCs at a density of 1 × 10^6 cells/ml were stimulated with 20 ng/ml PMA plus 500 ng/ml ionomycin for 6 h in the presence of GolgiStop (BD). Harvested PBMCs were washed and stained with PECy5-conjugated anti-human CD4 Ab (BioLegend) for 20 min at 4°C. Cells were washed three times and fixed and permeabilized with Cytofix/Cytoperm solution (BD) for 20 min at 4°C. Cells were then washed, incubated for 30 min with PE-conjugated anti-human IL-17A (BioLegend) or FITC-conjugated anti-human IFN-γ Abs (BioLegend), washed, and analyzed with a FACSCalibur (BD).

Results

A possible DBD mutation in STAT1

We first performed direct sequence analysis of the genes responsible for CMC in our patients: *AIRE*, *CLEC7A*, *CARD9*, *IL17RA*, *IL17F*, *IL2Rα*, and *STAT1* (4–6, 12–17). This study demonstrated that Patient 1 and Patient 2 have the same heterozygous base change in *STAT1* (c.1154C>T, p.T385M) (Fig. 1A), which was confirmed by the sequence analysis of TOPO-TA clones (Fig. 1B, data not shown). This base change has not been reported either as a mutation or as a single nucleotide polymorphism in the National Center for Biotechnology Information database, Ensembl database, or the Single Nucleotide Polymorphism Database, and it was not present in the family members of Patient 1 (Fig. 1C) or in 108 normal healthy controls (data not shown). Furthermore, the affected residue was evolutionarily conserved, as shown in Fig. 1D. The polymorphism phenotype-2 (PolyPhen-2) algorithm (http://genetics.bwh.harvard.edu/pph2/index.shtml), a structure sequence-based amino acid substitution-prediction method, predicted p.T385M as probably damaging, with a score of 1.000 (sensitivity: 0.00; specificity: 1.00). The sort intolerant from tolerant algorithm (http://sift.jcvi.org/) also predicted this amino acid substitution as deleterious. These results strongly indicate that c.1153C>T (p.T385M) is a de novo disease-causing mutation. Patient 1 was also shown to have an unreported heterozygous base change in *CARD9* (c.661G>A, p.K221E). However, this base change was also detected in his healthy father (data not shown). Additionally, PBMCs from Patient 1 showed normal IL-6 production in response

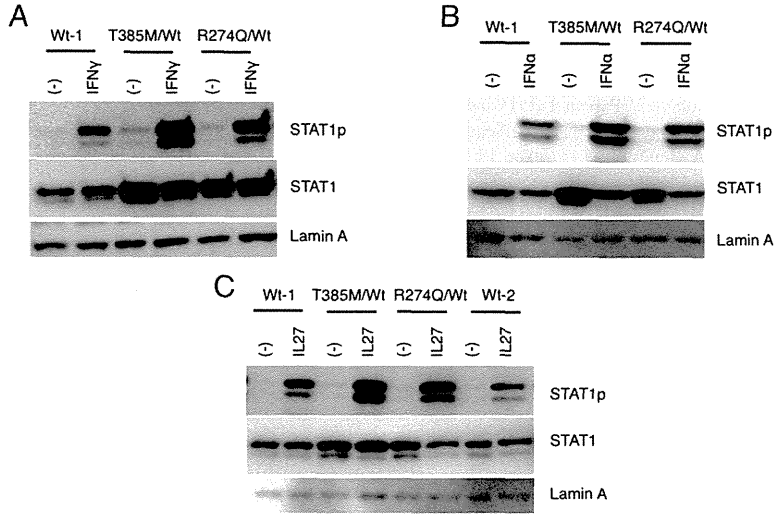

FIGURE 3. T385M was associated with hyperphosphorylation of STAT1 in response to IFN-γ, IFN-α, and IL-27 stimulation. Western blot analysis of STAT1p in nuclear extracts from EBV-LCLs was performed. Lamin A was used as a loading control. STAT1p expression in EBV-LCLs following IFN-γ (**A**), IFN-α (**B**), or IL-27 (**C**) stimulation for 30 min. (−), No stimulation.

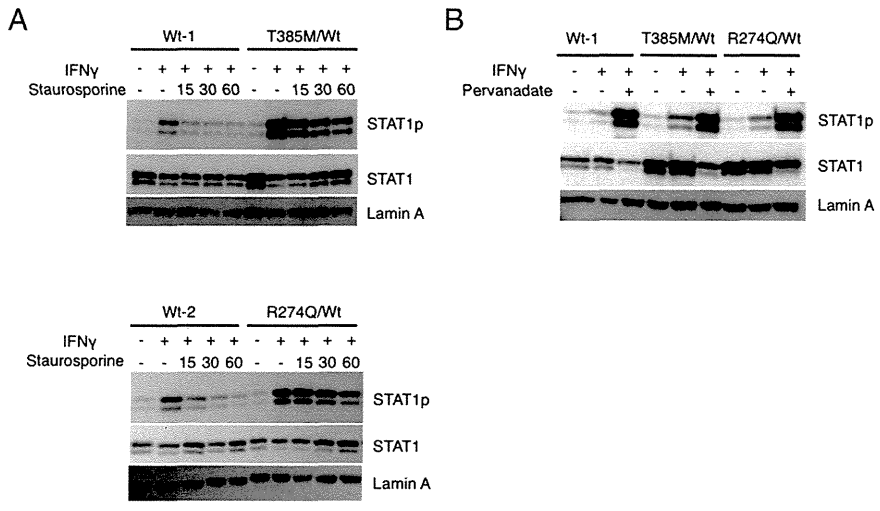

FIGURE 4. T385M was associated with hyperphosphorylation of STAT1 due to impaired dephosphorylation. (**A**) STAT1p expression in EBV-LCLs stimulated with IFN-γ for 30 min and then incubated with 1 μM staurosporine for 15, 30, or 60 min. (**B**) STAT1p expression in EBV-LCLs treated with pervanadate for 5 min and then stimulated with IFN-γ for 30 min.

to β-D-glucan stimulation with Curdlan (data not shown), indicating that the base change of c.661G>A, p.K221E in *CARD9* is not a disease-causing mutation but a single nucleotide polymorphism. The rest of the genes studied were demonstrated to be normal in both patients.

T385M is associated with gain of STAT1 function

Gain-of-function mutations in *STAT1* were very recently shown to be the genetic cause of autosomal-dominant or sporadic CMC (4–6). The reported mutations have been exclusively localized in the CC domain, leading to gain of STAT1 function due to impaired STAT1 dephosphorylation (4). To study whether the base change of c.1153C>T, p.T385M affecting the DBD of STAT1 also leads to gain of STAT1 function, the production of the downstream target of STAT1, IP-10, was studied following IFN-γ stimulation. IP-10 production was significantly higher in monocyte-derived macrophages from Patient 1 (T385M/Wt) and Patient 3 (R274Q/Wt) than in the matched control macrophages after IFN-γ–LPS stimulation (Fig. 2A). IP-10 production was also significantly higher in EBV-LCLs from Patient 1 (T385M/Wt) and Patient 3 (R274Q/Wt) after IFN-γ stimulation (Fig. 2B). These results indicated that T385M is a mutation leading to gain of STAT1 function.

STAT1 T385M leads to STAT1 hyperphosphorylation in response to IFN-γ, IFN-α, and IL-27 stimulation, which is due to impaired dephosphorylation

We then studied the STAT1 phosphorylation state in EBV-LCLs to determine the mechanisms of the gain of STAT1 function. Expression of phosphorylated STAT1 (STAT1p) protein following IFN-γ stimulation was higher in T385M/Wt and R274Q/Wt EBV-LCLs than in Wt EBV-LCLs (Fig. 3A). The hyperphosphorylated state of STAT1 was also observed following stimulation with IFN-α and IL-27 (Fig. 3B, 3C). Additionally, expression of total STAT1 in nuclear extract tends to be higher in T385M/Wt and R274Q/Wt EBV-LCLs than in Wt EBV-LCLs, especially without stimulation (Fig. 3). The mechanisms underlying STAT1 hyperphosphorylation in T385M/Wt EBV-LCLs were further explored with the tyrosine kinase inhibitor staurosporine and the phosphatase inhibitor pervanadate. The dephosphorylation of IFN-γ–ac-

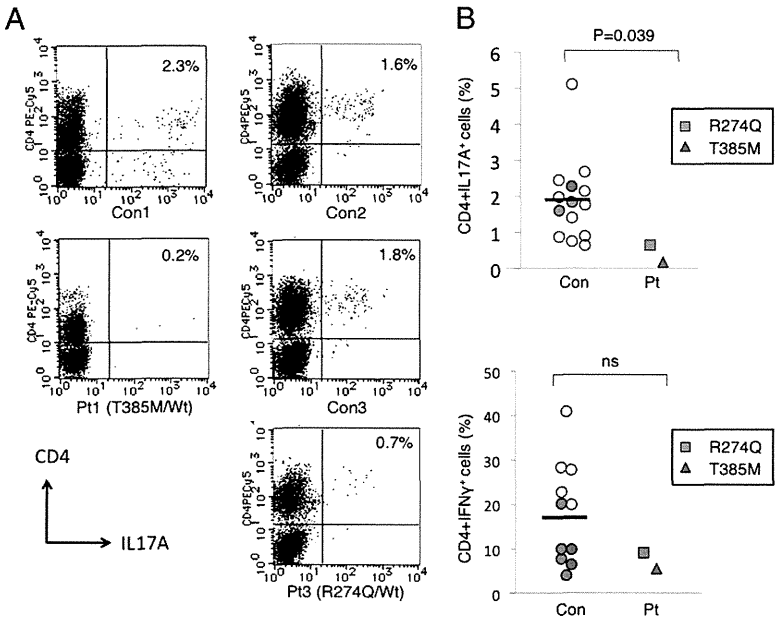

FIGURE 5. Patients 1 and 3 had deficient $CD4^+IL\text{-}17A^+$ cells but normal $CD4^+IFN\text{-}\gamma^+$ cells in response to PMA plus ionomycin stimulation. (**A**) Flow cytometric analysis of intracellular IL-17A expression following PMA plus ionomycin stimulation for 6 h. The proportion of $CD4^+IL\text{-}17A^+$ cells among $CD4^+$ cells was shown. (**B**) The proportion of $CD4^+IL\text{-}17A^+$ cells and $CD4^+IFN\text{-}\gamma^+$ cells among $CD4^+$ cells in normal controls and the patients. The horizontal lines indicate the mean proportion of $CD4^+IL\text{-}17A^+$ cells or $CD4^+IFN\text{-}\gamma^+$ cells in controls. Red and blue circles indicate controls obtained and analyzed at the same time as Patients 1 and 3, respectively. The *p* value was estimated using the Mann–Whitney *U* test. Con1, Control for Patient 1 obtained and analyzed at the same time; Con2 and Con3, controls for Patient 3 obtained and analyzed at the same time; Pt1, Patient 1; Pt3, Patient 3.

tivated T385M/Wt EBV-LCLs was impaired in the presence of staurosporine, as observed in R274Q/Wt EBV-LCLs (Fig. 4A). In contrast, with pervanadate treatment, the phosphorylation of STAT1 in T385M/Wt EBV-LCLs was similar to that seen in Wt EBV-LCLs (Fig. 4B). Therefore, the mechanisms underlying STAT1 hyperphosphorylation in T385M/Wt EBV-LCLs involve impaired dephosphorylation of STAT1, as observed in R274Q/Wt EBV-LCLs.

Patient 1 with the heterozygous T385M mutation in STAT1 had deficient Th17 cells

Deficient development of Th17 cells was documented to be associated with the development of CMC. CMC patients with gain-of-function mutations of *STAT1* affecting the CC domain have shown this defect (4). Therefore, we studied the proportion of $CD4^+IL\text{-}17A^+$ cells among $CD4^+$ cells in our patients after PMA plus ionomycin stimulation for 6 h. We also studied the population of $CD4^+IFN\text{-}\gamma^+$ cells to evaluate Th1 development. Patient 1 with the heterozygous T385M/Wt mutation of *STAT1* was reproducibly demonstrated to have dramatically reduced $CD4^+IL\text{-}17A^+$ cells (0.2% of $CD4^+$ cells), and Patient 3 with the heterozygous R274Q mutation had significantly reduced, but a little higher, $CD4^+IL\text{-}17A^+$ cells (0.7% of $CD4^+$ cells) (Fig. 5). The p value estimated using the Mann–Whitney U test was 0.039 between controls and the two patients. In contrast, both patients and controls had comparable percentages of $CD4^+IFN\text{-}\gamma^+$ cells (Fig. 5).

Discussion

To our knowledge, this study shows for the first time that the de novo heterozygous mutation of c.1153C>T in exon 14 (p.T385M), affecting the DBD of STAT1, is the genetic cause of sporadic CMC in two unrelated Japanese patients. The underlying mechanisms involve gain of STAT1 function due to impaired STAT1 dephosphorylation, as observed in the CC domain mutations (4).

Recent extensive studies of the STAT1 molecule reveal the association between the mutations affecting DBD and gain of STAT1 function. Based on crystallographic analysis, Darnell's group (7, 8) proposed a model of reorientation of phosphorylated "parallel" STAT1 dimers to an "antiparallel" form after leaving the DNA, which allows for reciprocal association of the CC domain and a pocket residue of the DBD for dephosphorylation. They further demonstrated in direct mutagenesis experiments that mutations of the pocket residues of the DBD, Q340A or Q340W, G384A or G384W, and Q408A or Q408W, resulted in impaired dephosphorylation of STAT1 (8). The fact that T385, the amino acid altered in two of our patients, is evolutionarily conserved and is positioned next to the pocket residue G384 may indicate that it is also critical in the reciprocal association with the CC domain for stabilizing the antiparallel structure and for dephosphorylation. It is also possible that this mutation of the DBD leads to impaired dissociation from the DNA, which may also cause a resistance to dephosphorylation of the STAT1 molecule. Higher expression of total STAT1 in nuclear extracts from T385M/Wt and R274Q/Wt EBV-LCLs than from Wt EBV-LCLs may reflect impaired nuclear export due to a resistance to dephosphorylation of the mutant STAT1 molecule (18), although the precise mechanisms were not determined in this study.

There may be more patients with CMC who carry gain-of-function mutations affecting the DBD of STAT1, given that significant numbers of patients with *STAT1* mutations are reported from all over the world (4–6). Additionally, crystallographic analysis and mutagenesis studies showed that mutations in the N-terminal domain (aa 1–130) also resulted in persistent phosphorylation (7, 8). This suggests that mutations affecting the N-terminal domain may also be a genetic cause of CMC.

We demonstrated deficient Th17 cells (0.2% of $CD4^+$ cells) in Patient 1 with the heterozygous T385M mutation, which was similar to or more severe than the defect observed in Patient 3 with the heterozygous R274Q mutation (0.7% of $CD4^+$ cells). Deficient development of Th17 cells may explain the increased susceptibility to *Candida* infection. IFN-γ, IFN-α, and IL-27 are potent inhibitors of Th17 cell development via STAT1 in mice and/or humans (19–21). Therefore, gain of STAT1 function in response to IFN-γ, IFN-α, or IL-27, which was observed in our patients, could be associated with deficient Th17 cell development. However, it remains to be determined precisely how gain of STAT1 function leads to deficient Th17 cells.

It is unclear whether there are differences in the clinical spectrum or severity of the disease between patients with the DBD mutations and the CC domain mutations. It might be worth noting that the two patients with the DBD mutation of T385M developed bronchiectasis in their early childhood, and one of them eventually developed HLH; these have not been described in patients with CC domain mutations.

With regard to HLH, administration of an anti–IFN-γ Ab was recently shown to have a therapeutic effect in two murine models of human hereditary HLH: perforin-deficient and Rab27a-deficient mice (22). Careful evaluation of the results indicates that T385M could be associated with higher expression of STAT1p in response to various stimulations (Fig. 3). Therefore, CMC patients with the DBD mutation of T385M may be more susceptible to the conditions presumably associated with enhanced IFN-γ–STAT1 signals, such as HLH. Detailed investigations of the clinical spectrum of these two populations should be conducted.

Acknowledgments

We thank Dr. D.M. Stewart (Metabolism Branch, National Cancer Institute, National Institutes of Health, Bethesda, MD) for reviewing the manuscript, the patients and their families for participation in this study, and Dr. H. Kanegane (Department of Pediatrics, Graduate School of Medicine, University of Toyama, Toyama, Japan) for coordinating patient recruitment.

Disclosures

The authors have no financial conflicts of interest.

References

1. Kirkpatrick, C. H. 1994. Chronic mucocutaneous candidiasis. *J. Am. Acad. Dermatol.* 31: S14–S17.
2. Mathis, D., and C. Benoist. 2009. Aire. *Annu. Rev. Immunol.* 27: 287–312.
3. Coleman, R., and R. J. Hay. 1997. Chronic mucocutaneous candidosis associated with hypothyroidism: a distinct syndrome? *Br. J. Dermatol.* 136: 24–29.
4. Liu, L., S. Okada, X. F. Kong, A. Y. Kreins, S. Cypowyj, A. Abhyankar, J. Toubiana, Y. Itan, M. Audry, P. Nitschke, et al. 2011. Gain-of-function human STAT1 mutations impair IL-17 immunity and underlie chronic mucocutaneous candidiasis. *J. Exp. Med.* 208: 1635–1648.
5. van de Veerdonk, F. L., T. S. Plantinga, A. Hoischen, S. P. Smeekens, L. A. Joosten, C. Gilissen, P. Arts, D. C. Rosentul, A. J. Carmichael, C. A. Smits-van der Graaf, et al. 2011. STAT1 mutations in autosomal dominant chronic mucocutaneous candidiasis. *N. Engl. J. Med.* 365: 54–61.
6. Smeekens, S. P., T. S. Plantinga, F. L. van de Veerdonk, B. Heinhuis, A. Hoischen, L. A. Joosten, P. D. Arkwright, A. Gennery, B. J. Kullberg, J. A. Veltman, et al. 2011. STAT1 hyperphosphorylation and defective IL12R/IL23R signaling underlie defective immunity in autosomal dominant chronic mucocutaneous candidiasis. *PLoS ONE* 6: e29248.
7. Zhong, M., M. A. Henriksen, K. Takeuchi, O. Schaefer, B. Liu, J. ten Hoeve, Z. Ren, X. Mao, X. Chen, K. Shuai, and J. E. Darnell, Jr. 2005. Implications of an antiparallel dimeric structure of nonphosphorylated STAT1 for the activation-inactivation cycle. *Proc. Natl. Acad. Sci. USA* 102: 3966–3971.
8. Mertens, C., M. Zhong, R. Krishnaraj, W. Zou, X. Chen, and J. E. Darnell, Jr. 2006. Dephosphorylation of phosphotyrosine on STAT1 dimers requires extensive spatial reorientation of the monomers facilitated by the N-terminal domain. *Genes Dev.* 20: 3372–3381.
9. Nagashima, T., A. Miyanoshita, Y. Sakiyama, Y. Ozaki, A. C. Stan, and K. Nagashima. 2000. Cerebral vasculitis in chronic mucocutaneous candidiasis: autopsy case report. *Neuropathology* 20: 309–314.

10. Yamada, M., Y. Okura, Y. Suzuki, S. Fukumura, T. Miyazaki, H. Ikeda, S. I. Takezaki, N. Kawamura, I. Kobayashi, and T. Ariga. 2012. Somatic mosaicism in two unrelated patients with X-linked chronic granulomatous disease characterized by the presence of a small population of normal cells. *Gene* 497: 110–115.
11. Schreiber, E., P. Matthias, M. M. Müller, and W. Schaffner. 1989. Rapid detection of octamer binding proteins with 'mini-extracts', prepared from a small number of cells. *Nucleic Acids Res.* 17: 6419.
12. Nagamine, K., P. Peterson, H. S. Scott, J. Kudoh, S. Minoshima, M. Heino, K. J. Krohn, M. D. Lalioti, P. E. Mullis, S. E. Antonarakis, et al. 1997. Positional cloning of the APECED gene. *Nat. Genet.* 17: 393–398.
13. Finnish-German APECED Consortium. 1997. An autoimmune disease, APECED, caused by mutations in a novel gene featuring two PHD-type zinc-finger domains. *Nat. Genet.* 17: 399–403.
14. Ferwerda, B., G. Ferwerda, T. S. Plantinga, J. A. Willment, A. B. van Spriel, H. Venselaar, C. C. Elbers, M. D. Johnson, A. Cambi, C. Huysamen, et al. 2009. Human dectin-1 deficiency and mucocutaneous fungal infections. *N. Engl. J. Med.* 361: 1760–1767.
15. Glocker, E. O., A. Hennigs, M. Nabavi, A. A. Schäffer, C. Woellner, U. Salzer, D. Pfeifer, H. Veelken, K. Warnatz, F. Tahami, et al. 2009. A homozygous CARD9 mutation in a family with susceptibility to fungal infections. *N. Engl. J. Med.* 361: 1727–1735.
16. Puel, A., S. Cypowyj, J. Bustamante, J. F. Wright, L. Liu, H. K. Lim, M. Migaud, L. Israel, M. Chrabieh, M. Audry, et al. 2011. Chronic mucocutaneous candidiasis in humans with inborn errors of interleukin-17 immunity. *Science* 332: 65–68.
17. Sharfe, N., H. K. Dadi, M. Shahar, and C. M. Roifman. 1997. Human immune disorder arising from mutation of the alpha chain of the interleukin-2 receptor. *Proc. Natl. Acad. Sci. USA* 94: 3168–3171.
18. McBride, K. M., C. McDonald, and N. C. Reich. 2000. Nuclear export signal located within theDNA-binding domain of the STAT1transcription factor. *EMBO J.* 19: 6196–6206.
19. Villarino, A. V., E. Gallo, and A. K. Abbas. 2010. STAT1-activating cytokines limit Th17 responses through both T-bet-dependent and -independent mechanisms. *J. Immunol.* 185: 6461–6471.
20. Ramgolam, V. S., Y. Sha, J. Jin, X. Zhang, and S. Markovic-Plese. 2009. IFN-beta inhibits human Th17 cell differentiation. *J. Immunol.* 183: 5418–5427.
21. Diveu, C., M. J. McGeachy, K. Boniface, J. S. Stumhofer, M. Sathe, B. Joyce-Shaikh, Y. Chen, C. M. Tato, T. K. McClanahan, R. de Waal Malefyt, et al. 2009. IL-27 blocks RORc expression to inhibit lineage commitment of Th17 cells. *J. Immunol.* 182: 5748–5756.
22. Pachlopnik Schmid, J., C. H. Ho, F. Chrétien, J. M. Lefebvre, G. Pivert, M. Kosco-Vilbois, W. Ferlin, F. Geissmann, A. Fischer, and G. de Saint Basile. 2009. Neutralization of IFNgamma defeats haemophagocytosis in LCMV-infected perforin- and Rab27a-deficient mice. *EMBO. Mol. Med.* 1: 112–124.

Molecular Genetics and Metabolism 105 (2012) 553–558

Contents lists available at SciVerse ScienceDirect

Molecular Genetics and Metabolism

journal homepage: www.elsevier.com/locate/ymgme

Simple and rapid genetic testing for citrin deficiency by screening 11 prevalent mutations in *SLC25A13*

Atsuo Kikuchi [a,*], Natsuko Arai-Ichinoi [a], Osamu Sakamoto [a], Yoichi Matsubara [b], Takeyori Saheki [c,1], Keiko Kobayashi [d], Toshihro Ohura [e], Shigeo Kure [a]

[a] *Department of Pediatrics, Tohoku University Graduate School of Medicine, 1-1 Seiryo-machi, Aoba-ku, Sendai, Miyagi 980-8574, Japan*
[b] *Department of Medical Genetics, Tohoku University School of Medicine, 1-1 Seiryo-machi, Aoba-ku, Sendai, Miyagi 980-8574, Japan*
[c] *Institute for Health Sciences, Tokushima Bunri University, 180 Yamashiro-cho, Tokushima 770-8514, Japan*
[d] *Department of Molecular Metabolism and Biochemical Genetics, Kagoshima University, Kagoshima 890-8544, Japan*
[e] *Division of Pediatrics, Sendai City Hospital, 3-1 Shimizukoji, Wakabayashi-ku, Sendai, Miyagi 984-8501, Japan*

ARTICLE INFO

Article history:
Received 13 November 2011
Received in revised form 29 December 2011
Accepted 30 December 2011
Available online 8 January 2012

Keywords:
Citrin deficiency
Genetic diagnosis
Rapid diagnosis
Expanded newborn screening
SLC25A13

ABSTRACT

Citrin deficiency is an autosomal recessive disorder caused by mutations in the *SLC25A13* gene and has two disease outcomes: adult-onset type II citrullinemia and neonatal intrahepatic cholestasis caused by citrin deficiency. The clinical appearance of these diseases is variable, ranging from almost no symptoms to coma, brain edema, and severe liver failure. Genetic testing for *SLC25A13* mutations is essential for the diagnosis of citrin deficiency because chemical diagnoses are prohibitively difficult. Eleven *SLC25A13* mutations account for 95% of the mutant alleles in Japanese patients with citrin deficiency. Therefore, a simple test for these mutations is desirable. We established a 1-hour, closed-tube assay for the 11 *SLC25A13* mutations using real-time PCR. Each mutation site was amplified by PCR followed by a melting-curve analysis with adjacent hybridization probes (HybProbe, Roche). The 11 prevalent mutations were detected in seven PCR reactions. Six reactions were used to detect a single mutation each, and one reaction was used to detect five mutations that are clustered in a 21-bp region in exon 17. To test the reliability, we used this method to genotype blind DNA samples from 50 patients with citrin deficiency. Our results were in complete agreement those obtained using previously established methods. Furthermore, the mutations could be detected without difficulty using dried blood samples collected on filter paper. Therefore, this assay could be used for newborn screening and for facilitating the genetic diagnosis of citrin deficiency, especially in East Asian populations.

1. Introduction

Citrin deficiency is an autosomal recessive disorder that results from mutations in the *SLC25A13* gene [1] and causes two diseases: adult-onset type II citrullinemia (CTLN2; OMIM #603471) and neonatal intrahepatic cholestasis caused by citrin deficiency (NICCD; OMIM#605814) [1–4]. The clinical appearance of these diseases is variable and ranges from almost no symptoms to coma, brain edema, and severe liver failure requiring transplantation [5–8]. In a study of patients with NICCD, only 40% of individuals were identified by newborn screenings to have abnormalities, such as hypergalactosemia, hypermethioninemia, and hyperphenylalaninemia [9]. Other patients were referred to hospitals with suspected neonatal hepatitis or biliary atresia, due to jaundice or discolored stool [9]. Hypercitrullinemia was not observed in all patients [9]. Mutation analysis of *SLC25A13* is indispensable because of the difficulties associated with the chemical diagnosis of citrin deficiency. The *SLC25A13* mutation spectrum in citrin deficiency is heterogeneous, and more than 31 mutations of *SLC25A13* have been identified to date [1,10–18]. However, there are several predominant mutations in patients from East Asia. As shown in Table 1, 6 prevalent mutations account for 91% of the mutant alleles in the Japanese population [12,19]. Five additional mutations also occur within a 21-bp cluster in exon 17 (Table 1 and Fig. 1D). The six prevalent mutations, together with the five mutations in exon 17, account for 95% of the mutant alleles in Japan [12,19].

Several different methods, such as direct sequencing, PCR restriction fragment length polymorphism (PCR-RFLP), and denaturing high performance liquid chromatography (DHPLC), are currently used for the detection of mutations in *SLC25A13* [1,10–14,19]. However, these methods are too complex for clinical use. Direct sequencing is a standard but cumbersome method. The PCR-RFLP method is

Abbreviations: CTLN2, adult-onset type II citrullinemia; FRET, fluorescence resonance energy transfer; HRM, high resolution melting; NICCD, neonatal intrahepatic cholestasis caused by citrin deficiency; Tm, melting temperature.

* Corresponding author. Fax: +81 22 717 7290.
E-mail address: akikuchi-thk@umin.ac.jp (A. Kikuchi).
[1] Present address: Institute of Resource Development and Analysis, Kumamoto University, Kumamoto 860-0811, Japan.

1096-7192/$ – see front matter © 2012 Elsevier Inc. All rights reserved.
doi:10.1016/j.ymgme.2011.12.024

Table 1
Seven primer/probe sets and 11 targeted mutations of *SLC25A13*.

Primer/probe set	Mutation		Location	Nucleotide change	Effects of mutations	Allele frequency*[19]	References
A	Mutation [I]	:851del4	exon 9	c.851_854delGTAT	p.R284fs(286X)	33.2%	[1]
B	Mutation [II]	:g.IVS11+1G>A	intron 11	c.1019_1177del	p.340_392del	37.6%	[1]
C	Mutation [III]	:1638ins23	exon 16	c.1638_1660dup	p.A554fs(570X)	3.4%	[1]
D	Mutation [IV]	:S225X	exon 7	c.675C>A	p.S225X	5.3%	[1]
E	Mutation [V]	:g.IVS13+1G>A	intron 13	c.1231_1311del	p.411_437del	8.2%	[1]
F	Mutation [XIX]	:IVS16ins3kb	intron 16	c. aberrant RNA	p.A584fs(585X)	4.6%	[19]
G	Mutation [VI]	:1800ins1	exon 17	c.1799_1800insA	p.Y600X	1.3%	[10]
	Mutation [VII]	:R605X	exon 17	c.1813C>T	p.R605X	0.90%	[10]
	Mutation [VIII]	:E601X	exon 17	c.1801G>T	p.E601X	1.2%	[11]
	Mutation [IX]	:E601K	exon 17	c.1801G>A	p.E601K	0.30%	[11]
	Mutation [XXI]	:L598R	exon 17	c.1793T>G	p.L598R	0%	[15]
						Total 95.1%	

* The frequency of each mutant allele among Japanese patients with citrin deficiency.

complicated and can lead to genotyping errors, due to incomplete digestion by the restriction enzymes. DHPLC is time-consuming and requires expensive equipment. Thus, there is a strong need for the development of a simple test for these mutations.

The goal of this study was to establish a rapid and simple test for the detection of the 11 most common *SLC25A13* mutations. We adopted the HybProbe format (Roche) for the detection of the mutations using real-time PCR followed by a melting-curve analysis with adjacent hybridization probes [20,21]. This assay can be completed in less than 1 h and has the advantage of being a closed-tube assay. The fundamental process for detecting point mutations using the HybProbe assay is presented in Fig. 1A. The 11 prevalent mutations contain not only point mutations but also include a 4-bp deletion and insertions of 1-bp, 23-bp and 3-kb genomic fragments (Table 1 and Fig. 1). Careful design of the PCR primers and HybProbes enabled us to test for these various *SLC25A13* mutations.

2. Methods

2.1. Subjects

CTLN2 and NICCD were diagnosed, as previously described [9,10,19,22–24]. Genomic DNA of the patients was obtained from peripheral blood leukocytes using the DNeasy blood kit (Qiagen Inc., Valencia, CA, USA). Genomic DNA was purified from filter paper blood samples using the ReadyAmp Genomic DNA Purification System (Promega, Madison, WI, USA). Mutations in these DNA samples were analyzed at Kagoshima University using a combination of PCR with or without restriction enzyme digestion or by direct sequencing, as previously described [1,10–14,19]. Another set of samples was obtained from 420 healthy volunteers (mainly from Miyagi prefecture in the northeastern region of Japan) at Tohoku University. Genomic DNA from leukocytes was extracted, as described above.

2.2. Detection of seven prevalent mutations in SLC25A13 using the HybProbe assay

HybProbe probes comprise a pair of donor and acceptor oligonucleotide probes designed to hybridize adjacent to their target sites in an amplified DNA fragment [20,21]. The donor probes are labeled at their 3′ end with fluorescein isothiocyanate (FITC), whereas the acceptor probes are labeled at their 5′ end with LC Red640; these acceptor probes are phosphorylated at their 3′ end to prevent extension by the DNA polymerase. When two probes hybridize to the amplicon, the fluorescent dyes are located within 5 bases of each other, which allows fluorescence resonance energy transfer (FRET) between the excited FITC and the LC Red640; this process emits light that can be quantified by real-time PCR. Following PCR amplification, a melting-peak analysis is performed. The melting peak is produced by the reporter probe, which has a lower melting temperature (Tm) than the other probe, called the anchor probe. As the reporter melts from the target, the fluorophores are separated, and the FRET ceases. The Tm of the reporter probe determines the reaction

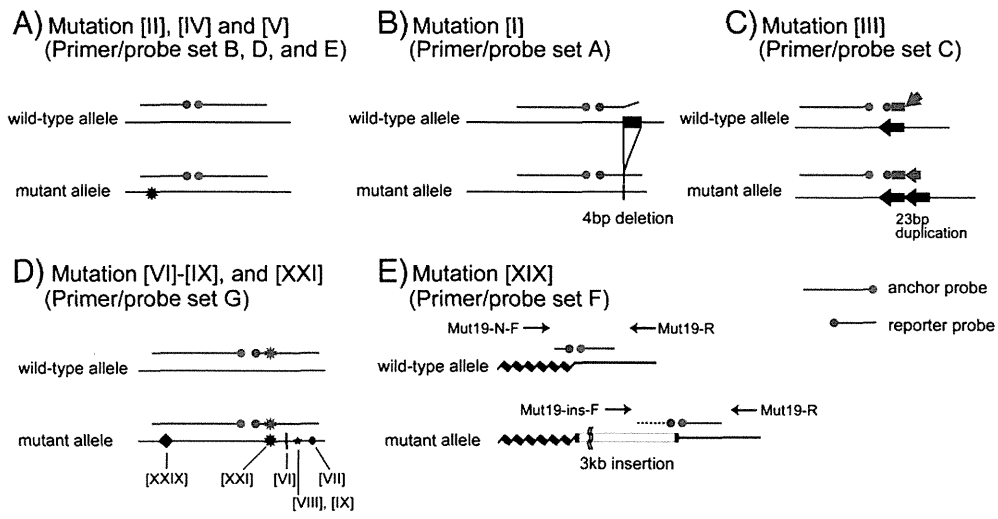

Fig. 1. Principle of *SLC25A13* mutation detection by melting-curve analysis with the HybProbe assay. In primer/probe sets A–E, and G, PCR was performed with a pair of primers, whereas in primer/probe set F, two forward primers and one common reverse primer were used for the amplification of both wild-type and mutant alleles. Note that mutation [XXIX], located on the anchor probe of primer/probe set G, is a non-target mutation.

specificity (i.e., binding of the probe to a perfectly matched sequence rather than to regions with sequence mismatches).

Seven primer/probe sets were designed for this study. Fig. 1 shows a schematic diagram of the strategy for mutation detection using these primer/probe sets. Tables 1 and 2 list the primer/probe sets and corresponding sequences and primer concentrations that were used to target the 11 mutations. Primer/probe sets A, B, C, D, E, and F were designed to detect mutations [I], [II], [III], [IV], [V], and [XIX], respectively. Primer/probe set G was designed to detect the five mutations clustered on exon 17: mutations [VI], [VII], [VIII], [IX], and [XXI] (Fig. 1D). All primers and probes were synthesized based on the NCBI reference SLC25A13 gene sequence (GenBank accession no. **NM_014251**) with the exception of mutation [XIX]:IVS16ins3kb, which was designed according to [19].

Real-time PCR and subsequent melting curve analyses were performed in a closed tube using a 20-μL mixture on a LightCycler 1.5 (Roche Diagnostics, Tokyo, Japan). The PCR mixture contained 2.0 μL of genomic DNA (10–50 ng), 0.5 μM of forward primer, 0.5 or 0.1 μM of reverse primer, 0.2 μM of each sensor and anchor probe, and 10 μL of Premix ExTaq™ (Perfect Real Time) reagent (TaKaRa Bio Inc., Otsu, Japan).

The thermal profile conditions were identical for all seven assays and consisted of an initial denaturation step (30 s at 95 °C), followed by 45 amplification cycles with the following conditions: denaturation for 5 s at 95 °C and annealing and extension for 20 s at 60 °C. The transition rate between all steps was 20 °C/s. After amplification, the samples were held at 37 °C for 1 min, followed by the melting curve acquisition at a ramp rate of 0.15 °C/s extending to 80 °C with continuous fluorescence acquisition.

Table 2
Primers, probes and target amplicon sequences, target mutation sites, and primer concentrations.

Primer/probe set	Name	Sequences of PCR products, primer locations, probe sequences, and mutation sites (5′ to 3′)	Concentration (μmol/L)
A		GGCTATACTGAAATATGAGAAatgaaaaagggatgtttttaaatttataatgtaaattgtaataaattggtatatttgttgcttgtgtttgtttttcccctacagac	
		gtatgaccttagcagacattgaacggattgctcctctggaagagggaactctgccCTTTAACTTGGCTGAGG (181 bp)	
	Mut1-F	GGCTATACTGAAATATGAGAA	0.5
	Mut1-R	CCTCAGCCAAGTTAAAG	0.5
	Mut1-UP	ATGTAAATTGTAATAAATTGGTATATTTGTTGCTTGTGTT-FITC	
	Mut1-DW	LC Red640-GTTTTTCCCCTACAGAC**GACC**-P	
B		GAATGCAGAACCAACGAtcaactggctcttttgtgggagaactcatgtataaaaacagctttgactgttttaagaaagtgctacgctatgaaggcttctt	
		tggactgtatagaggttagtgccacatgctcaatacctgttaggtgaaataacactcaaaggtttggtttctcatcttagtgcctGACATGAATTAGCAAGACTG (205 bp)	
	Mut2-F	GAATGCAGAACCAACGA	0.5
	Mut2-R	CAGTCTTGCTAATTCATGTC	0.1
	Mut2-UP	ACCTAACAGGTATTGAGCATGTG-FITC	
	MUt2-DW	LC Red640-CACTAA**CC**TCTATACAGTCCA-P	
C		GCAGTTCAAAGCACAGTTATTtttatatagtgagaatgtgaccagactgagatggtgttgtgtctctcctgcaggtatgcctgcagcatctttagtg	
		accgctgatgttatcaagacgagattacaggtg	
		gctgcccggg(**gagatta**caggtggctgcccggg)ctggccaaaccaCTTACAGCGGAGTGATAGAC (175 bp)	
	Mut3-F	GCAGTTCAAAGCACAGTTATT	0.5
	Mut3-R	GTCTATCACTCCGCTGTAAG	0.5
	Mut3-UP	ACCCCTGCTGATGTTATCAAGACGAGATTACAGGT-FITC	
	Mut3-DW	LC Red640-GCTGCCCGGG**GAGATTA**-P	
D		TCAATTTATTTGAGGCTGCtggaggtaccacatcccatcaagttagtttctcctattttaatggatttaatt**c**gctccttaacaac	
		atggaactcattagaaagatctatagcactc	
		tggctggcaccaggaaagatgttgaagtGACTAAGGGTGAGTGAGAA (164 bp)	
	Mut4-F	TCAATTTATTTGAGGCTGC	0.5
	Mut4-R	TTCTCACTCACCCTTAGTC	0.5
	Mut4-UP	AATGGATTTAATT**C**GCTCCTTAACA-FITC	
	Mut4-DW	LC Red640-ATGGAACTCATTAGAAAGATCTATAGCACTC-P	
E		TGCACAAAGATGGTTCGgtcccacttgcagcagaaattcttgctggaggctgc**g**taagtacctttgaagctctcttcattgaaaagacttgtttcac	
		atatatatcactaccatggtcaacaggtgtggactaaggcttctgttTAACCACAGATCCTGCA (162 bp)	
	Mut5-F	TGCACAAAGATGGTTCG	0.5
	Mut5-R	TGCAGGATCTGTGGTTA	0.5
	Mut5-UP	GTGAAACAAGTCTTTTCAATGAAGAGAGCTTC-FITC	
	Mut5-DW	LC Red640-AAGGTACTTA**C**GCAGCCTC-P	
F	normal allele	GGAGCTGGTGGTATGGAAataatgtgttcttaactaactctttggtatcaggtaaatttttaaaatatctaattatatctgtgatttctc	
		catttttttaaagctcgtgtatttcgatcctcaccccagtttggt	
		gtaactttgctgacttacgaattgctacagcgatggttctacattgattttggaggagtgtaagtatcatgctaaatctgctgctaaatttt	
		GGCTGCTGCTAATGCTC (244 bp)	
	insertion allele	CCATCTTCCTCCTCCCTTggcagccccgccccccgatttctccatttttttaaagctcgtgtatttcgatcctcaccccagtttggt	
		gtaactttgctgacttacgaattgctacagcgatggttctacattgatttt	
		ggaggagtgtaagtatcatgctaaatctgctgctaaattttGGCTGCTGCTAATGCTC (196 bp)	
	Mut19-N-F	GGAGCTGGTGGTATGGAA	0.5
	Mut19-ins-F	CCATCTTCCTCCTCCCTT	0.5
	Mut19-R	GAGCATTAGCAGCAGCC	0.5
	Mut19-UP	ACCAAACTGGGGTGAGGATCGAAATACACGAGCTTTAAAAAAATG-FITC	
	Mut19-N-DW	LC Red640-AGAAATCACAGATATAATTAGATATTT-P	
	Mut19-ins-DW	LC Red640-AGAAATCGGGGGGCGGGG-P	
G		TCTTAACTAACTCTTTGGTATCAGGTaaatttttaaaatatctaattatatctgtgatttctccatttttttaaagctcg	
		tgtatttcgatcctcaccccagtttggtgtaactttg**c**t**g**actt**a(a)cg**aattgctacag**c**ga	
		tggttctacattgattttggaggagtgtaagtatcatgctaaatctgctgctaaattttGGCTGCTGCTAATGCTC (217 bp)	
	Mut6-9, 21-F	TCTTAACTAACTCTTTGGTATCAGGT	0.5
	Mut6-9, 21-R	GAGCATTAGCAGCAGCC	0.5
	Mut6-9, 21-UP	TGTATTTCGATCCTCACCCCAGTTTGGTGTAACTT-FITC	
	Mut6-9, 21-DW	LC Red640-GC**G**GACTT**ACG**AATTGCTACAG**C**GA-P	

Upper case and underlined letters indicate the locations of primers and probes, respectively. Inserted DNA is shown in parenthesis. Nucleotides in boldface were used for mutation detection.
F: forward, R: reverse, UP: upstream, DW: downstream, N: normal allele, ins: insertion allele, FITC: fluorescein isothiocyanate, P: phosphate.

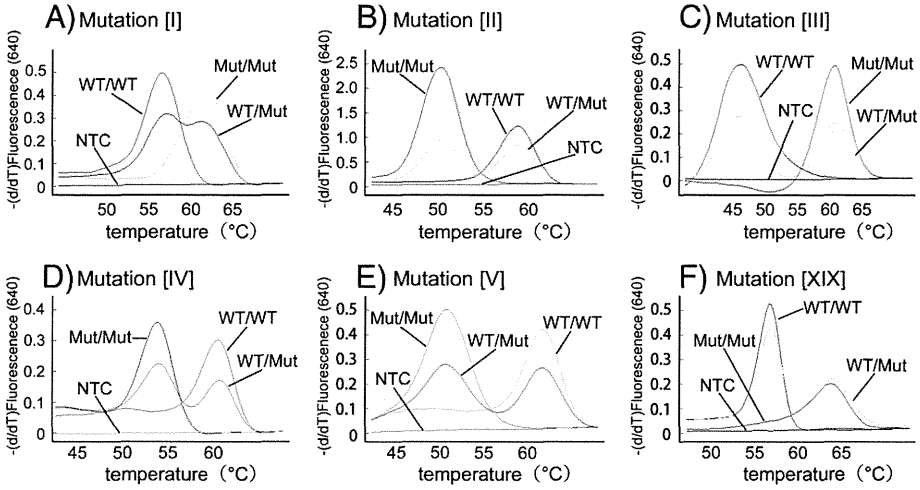

Fig. 2. Typical melting curves used in the detection of mutations [I–V] and [XIX]. Each assay using primer/probe sets A–F is displayed in a separate graph (A–F). WT: wild-type allele, Mut: mutant allele, NTC: no DNA template control.

2.3. Validation of the mutation detection system

After establishing the protocol for detecting the 11 prevalent mutations, 50 DNA samples from patients' blood were sent from Kagoshima University to Tohoku University for the validation of this system in a single-blind manner. Similarly, 26 DNA samples purified from paper-filter blood samples were analyzed in the same manner as the blood DNA samples.

2.4. Estimation of the carrier frequency

For the estimation of the heterozygous carrier frequency, 420 genomic DNA samples from healthy volunteers were screened using the HybProbe analysis for the 11 prevalent mutations. All detected mutations were confirmed by direct sequencing.

2.5. Ethics

This study was approved by the Ethical Committees of Tohoku University School of Medicine and Kagoshima University. Written informed consent was obtained from all participants or their guardians.

3. Results

3.1. Development of the mutation detection system

In primer/probe sets B, D, and E, the reporter probes were designed to be complimentary to the wild-type allele (Fig. 1A). To allow for an improved detection of the mutations, primer/probe sets A and C were designed to be complementary to the mutant allele (Figs. 1B, C). In the primer/probe set F, two forward PCR primers, which were specific to the wild-type and the mutant alleles, were used with a common reverse primer for the co-amplification of the wild-type and 3-kb insertion alleles (Fig. 1E). Two reporter probes, which had a common anchor probe, were used for the detection of the wild-type and mutant alleles. Because the two reporter probes had different melting temperatures, we were able to identify the allele that was amplified. Fig. 2 shows representative results of the melting curve analyses using the primer/probe sets A–F, in which all of the mutant alleles generated distinct peaks corresponding to the wild-type alleles.

In the primer/probe set G, we used a reporter probe that was complementary to the mutant [XXI] allele (Fig. 1D). All five mutations in exon 17 were successfully differentiated from the wild-type allele (Figs. 3A–E). The [XXIX] mutation is an additional mutation in exon

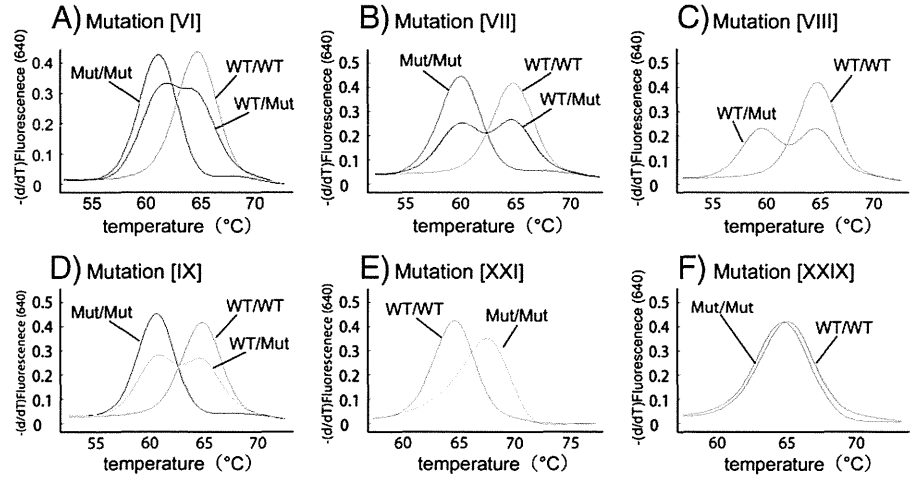

Fig. 3. Typical melting curves used in the detection of mutations [VI–XI], [XXI], and [XXIX] on exon 17. Genotyping was performed using primer/probe set G. Each melting curve for a target mutation is displayed in a separate graph (A–F). Note that mutation [XXIX] (F) is a non-target mutation on the anchor probe. WT: wild-type allele, Mut: mutant allele.

17 that is not listed in Table 1. The [XXIX] mutation is located in the anchor-probe binding site and not on the reporter-probe binding site (Fig. 1D). To examine the effect of mutations on the anchor probe, we genotyped a patient with a heterozygous [XXIX] mutation using primer/probe set G (Fig. 3F). We found no change in the melting curves between the wild-type allele and the [XXIX] allele, thereby suggesting that point mutations within the anchor probe sequence have little effect on the melting curve analysis.

3.2. Validation

The genotypes determined at Tohoku University using the proposed method and those determined at Kagoshima University using a previously published method were identical for the 11 common mutations (Table S1 in supplementary material). We performed a similar test using DNA samples purified from filter-paper blood samples to determine if this method could be used for newborn screening. The genotypes determined in both laboratories were identical for all 26 DNA samples (Table S2 in supplementary material).

3.3. Frequency of eleven prevalent mutations

We found four heterozygous carriers of mutation [I], three of mutation [II], and two of mutation [V]. In addition, primer/probe set G detected one heterozygous mutation, which was confirmed as mutation [VIII] by direct sequencing. Altogether, 10 mutations were detected in 420 Japanese healthy controls.

4. Discussion

We developed a simple and rapid genetic test using real-time PCR combined with the HybProbe system for the 11 prevalent mutations in *SLC25A13*: mutations [I], [II], [III], [IV], [V], [VI], [VII], [VIII], [IX], [XIX], and [XXI]. This genetic test is a closed-tube assay in which no post-PCR handling of the samples is required. In addition, the genotyping is completed within 1 h. This test can utilize DNA samples purified from both peripheral blood and filter-paper blood. The reliability of the test was confirmed by genotyping 76 blind DNA samples from patients with citrin deficiency, including 50 peripheral blood and 26 filter-paper blood DNA samples. Because screening for the 11 targeted mutations would identify 95% of mutant alleles in the Japanese population [19], both, one, and no mutant alleles are expected to be identified in 90.4%, 9.3%, and less than 0.3% of patients, respectively. This genetic test would be useful not only in Japan but also other East Asian countries, including China, Korea, Taiwan and Vietnam, in which the same mutations are prevalent. Our test is expected to detect 76–87% of the mutant alleles in the Chinese population [12,19,25], 95–100% in the Korean population [12,19,26], 60–68% in the Taiwanese population [27,28], and 100% in the Vietnamese population [12,19]. If we were to prepare a primer/probe set for mutation [X]:g.IVS6+5G>A [12], which is prevalent in Taiwan, the estimated sensitivity would exceed 90% in the Taiwanese population [27,28].

Recently, the high resolution melting (HRM) method was reported to be suitable for the screening of mutations in the diagnosis of citrin deficiency [28]. HRM analysis is a closed-tube assay that screens for any base changes in the amplicons. The presence of SNPs anywhere on the amplicons can affect the melting curve, thereby suggesting that HRM is not suitable for screening for known mutations, but rather, is best suited to screening for unknown mutations. When we detected one heterozygous prevalent mutation, we performed HRM screening for all 17 exons of *SLC25A13*. After HRM screening, only the HRM-positive exons were subjected to direct sequencing analysis. Several mutant alleles were identified using this approach.

The frequency of homozygotes, including compound heterozygotes, presenting *SLC25A13* mutations in the population at Kagoshima (a prefecture in the southern part of Japan) has been calculated to be 1/17,000 based on the carrier rate (1/65) [19]. The prevalence of NICCD has been also reported to be 1/17,000–34,000 [29]. In this study, the carrier rate in Miyagi (a prefecture in northern Japan) was 1/42 (95% confidential interval, 1/108–1/26), thereby yielding an estimated frequency of patients with citrin deficiency of 1/7,100. Our result, together with the previous report [19], suggests that a substantial fraction of the homozygotes or compound heterozygotes of SLC25A13 mutations was asymptomatic during the neonatal period.

The early and definitive diagnosis of citrin deficiency may be beneficial for patients with citrin deficiency by encouraging specific dietary habits and avoiding iatrogenic worsening of brain edema by glycerol infusion when patients develop encephalopathy [30,31]. Because the screening of blood citrulline levels by tandem mass analysis at birth does not detect all patients with citrin deficiency, the development of a genetic test would be welcomed. In this study, we demonstrated that genomic DNA extracted from filter paper blood samples was correctly genotyped, thereby indicating the feasibility of newborn screening using this genetic test. If 100,000 babies in the northern part of Japan were screened by this method, we would detect 14 homozygotes or compound heterozygotes with *SLC25A13* mutations and 2400 heterozygous carriers. In 2400 heterozygous carriers, we would expect to observe only 1 to 2 compound heterozygotes with one target and one non-target mutation. The estimated frequency of babies with two non-target mutations is 0.04/100,000. Our genetic method would therefore allow us to screen newborn babies efficiently. If we performed this genetic test in a high-throughput real-time PCR system, such as a 384- or 1,536-well format, the cost per sample could be lowered.

In conclusion, we have established a rapid and simple detection system using the HybProbe assay for the 11 prevalent mutations in *SLC25A13*. This system could be used to screen newborns for citrin deficiency and may facilitate the genetic diagnosis of citrin deficiency, especially in East Asian populations.

Supplementary materials related to this article can be found online at doi:10.1016/j.ymgme.2011.12.024.

Acknowledgments

The authors acknowledge the contribution of Dr. Keiko Kobayashi, who passed away on December 21th, 2010. Dr. Kobayashi discovered that the *SLC25A13* gene is responsible for citrin deficiency and devoted much of her life to elucidating the mechanism of citrin deficiency. This work was supported by grants from the Ministry of Education, Culture, Sports, Science, and Technology and the Ministry of Health, Labor, and Public Welfare.

References

[1] K. Kobayashi, D.S. Sinasac, M. Iijima, A.P. Boright, L. Begum, J.R. Lee, T. Yasuda, S. Ikeda, R. Hirano, H. Terazono, M.A. Crackower, I. Kondo, L.C. Tsui, S.W. Scherer, T. Saheki, The gene mutated in adult-onset type II citrullinaemia encodes a putative mitochondrial carrier protein, Nat. Genet. 22 (1999) 159–163.
[2] T. Ohura, K. Kobayashi, Y. Tazawa, I. Nishi, D. Abukawa, O. Sakamoto, K. Iinuma, T. Saheki, Neonatal presentation of adult-onset type II citrullinemia, Hum. Genet. 108 (2001) 87–90.
[3] Y. Tazawa, K. Kobayashi, T. Ohura, D. Abukawa, F. Nishinomiya, Y. Hosoda, M. Yamashita, I. Nagata, Y. Kono, T. Yasuda, N. Yamaguchi, T. Saheki, Infantile cholestatic jaundice associated with adult-onset type II citrullinemia, J. Pediatr. 138 (2001) 735–740.
[4] T. Tomomasa, K. Kobayashi, H. Kaneko, H. Shimura, T. Fukusato, M. Tabata, Y. Inoue, S. Ohwada, M. Kasahara, Y. Morishita, M. Kimura, T. Saheki, A. Morikawa, Possible clinical and histologic manifestations of adult-onset type II citrullinemia in early infancy, J. Pediatr. 138 (2001) 741–743.
[5] T. Shigeta, M. Kasahara, T. Kimura, A. Fukuda, K. Sasaki, K. Arai, A. Nakagawa, S. Nakagawa, K. Kobayashi, S. Soneda, H. Kitagawa, Liver transplantation for an

infant with neonatal intrahepatic cholestasis caused by citrin deficiency using heterozygote living donor, Pediatr. Transplant. 14 (2009) E86–88.
[6] M. Kasahara, S. Ohwada, T. Takeichi, H. Kaneko, T. Tomomasa, A. Morikawa, K. Yonemura, K. Asonuma, K. Tanaka, K. Kobayashi, T. Saheki, I. Takeyoshi, Y. Morishita, Living-related liver transplantation for type II citrullinemia using a graft from heterozygote donor, Transplantation 71 (2001) 157–159.
[7] Y. Takashima, M. Koide, H. Fukunaga, M. Iwai, M. Miura, R. Yoneda, T. Fukuda, K. Kobayashi, T. Saheki, Recovery from marked altered consciousness in a patient with adult-onset type II citrullinemia diagnosed by DNA analysis and treated with a living related partial liver transplantation, Intern. Med. 41 (2002) 555–560.
[8] A. Tamamori, Y. Okano, H. Ozaki, A. Fujimoto, M. Kajiwara, K. Fukuda, K. Kobayashi, T. Saheki, Y. Tagami, T. Yamano, Neonatal intrahepatic cholestasis caused by citrin deficiency: severe hepatic dysfunction in an infant requiring liver transplantation, Eur. J. Pediatr. 161 (2002) 609–613.
[9] T. Ohura, K. Kobayashi, Y. Tazawa, D. Abukawa, O. Sakamoto, S. Tsuchiya, T. Saheki, Clinical pictures of 75 patients with neonatal intrahepatic cholestasis caused by citrin deficiency (NICCD), J. Inherit. Metab. Dis. 30 (2007) 139–144.
[10] T. Yasuda, N. Yamaguchi, K. Kobayashi, I. Nishi, H. Horinouchi, M.A. Jalil, M.X. Li, M. Ushikai, M. Iijima, I. Kondo, T. Saheki, Identification of two novel mutations in the SLC25A13 gene and detection of seven mutations in 102 patients with adult-onset type II citrullinemia, Hum. Genet. 107 (2000) 537–545.
[11] N. Yamaguchi, K. Kobayashi, T. Yasuda, I. Nishi, M. Iijima, M. Nakagawa, M. Osame, I. Kondo, T. Saheki, Screening of SLC25A13 mutations in early and late onset patients with citrin deficiency and in the Japanese population: identification of two novel mutations and establishment of multiple DNA diagnosis methods for nine mutations, Hum. Mutat. 19 (2002) 122–130.
[12] Y.B. Lu, K. Kobayashi, M. Ushikai, A. Tabata, M. Iijima, M.X. Li, L. Lei, K. Kawabe, S. Taura, Y. Yang, T.-T. Liu, S.-H. Chiang, K.-J. Hsiao, Y.-L. Lau, L.-C. Tsui, D.H. Lee, T. Saheki, Frequency and distribution in East Asia of 12 mutations identified in the SLC25A13 gene of Japanese patients with citrin deficiency, J. Hum. Genet. 50 (2005) 338–346.
[13] E. Ben-Shalom, K. Kobayashi, A. Shaag, T. Yasuda, H.-Z. Gao, T. Saheki, C. Bachmann, O. Elpeleg, Infantile citrullinemia caused by citrin deficiency with increased dibasic amino acids, Mol. Genet. Metab. 77 (2002) 202–208.
[14] J. Takaya, K. Kobayashi, A. Ohashi, M. Ushikai, A. Tabata, S. Fujimoto, F. Yamato, T. Saheki, Y. Kobayashi, Variant clinical courses of 2 patients with neonatal intrahepatic cholestasis who have a novel mutation of SLC25A13, Metab. Clin. Exp. 54 (2005) 1615–1619.
[15] A. Luder, A. Tabata, M. Iijima, K. Kobayashi, H. Mandel, Citrullinaemia type 2 outside East Asia: Israeli experience, J. Inherit. Metab. Dis. 29 (2006) 59.
[16] T. Hutchin, M. Preece, K. Kobayashi, T. Saheki, R. Brown, D. Kelly, P. McKiernan, A. Green, U. Baumann, Neonatal intrahepatic cholestasis caused by citirn deficiency (NICCD) in a European patient, J. Inherit. Metab. Dis. 29 (2006) 112.
[17] J.-S. Sheng, M. Ushikai, M. Iijima, S. Packman, K. Weisiger, M. Martin, M. McCracken, T. Saheki, K. Kobayashi, Identification of a novel mutation in a Taiwanese patient with citrin deficiency, J. Inherit. Metab. Dis. 29 (2006) 163.
[18] J.M. Ko, G.-H. Kim, J.-H. Kim, J.Y. Kim, J.-H. Choi, M. Ushikai, T. Saheki, K. Kobayashi, H.-W. Yoo, Six cases of citrin deficiency in Korea, Int. J. Mol. Med. 20 (2007) 809–815.
[19] A. Tabata, J.-S. Sheng, M. Ushikai, Y.-Z. Song, H.-Z. Gao, Y.-B. Lu, F. Okumura, M. Iijima, K. Mutoh, S. Kishida, T. Saheki, K. Kobayashi, Identification of 13 novel mutations including a retrotransposal insertion in SLC25A13 gene and frequency of 30 mutations found in patients with citrin deficiency, J. Hum. Genet. 53 (2008) 534–545.
[20] P.S. Bernard, R.S. Ajioka, J.P. Kushner, C.T. Wittwer, Homogeneous multiplex genotyping of hemochromatosis mutations with fluorescent hybridization probes, Am. J. Pathol. 153 (1998) 1055–1061.
[21] C.N. Gundry, P.S. Bernard, M.G. Herrmann, G.H. Reed, C.T. Wittwer, Rapid F508del and F508C assay using fluorescent hybridization probes, Genet. Test. 3 (1999) 365–370.
[22] T. Saheki, K. Kobayashi, I. Inoue, Hereditary disorders of the urea cycle in man: biochemical and molecular approaches, Rev. Physiol. Biochem. Pharmacol. 108 (1987) 21–68.
[23] K. Kobayashi, M. Horiuchi, T. Saheki, Pancreatic secretory trypsin inhibitor as a diagnostic marker for adult-onset type II citrullinemia, Hepatology 25 (1997) 1160–1165.
[24] Y. Tazawa, K. Kobayashi, D. Abukawa, I. Nagata, S. Maisawa, R. Sumazaki, T. Iizuka, Y. Hosoda, M. Okamoto, J. Murakami, S. Kaji, A. Tabata, Y.B. Lu, O. Sakamoto, A. Matsui, S. Kanzaki, G. Takada, T. Saheki, K. Iinuma, T. Ohura, Clinical heterogeneity of neonatal intrahepatic cholestasis caused by citrin deficiency: case reports from 16 patients, Mol. Genet. Metab. 83 (2004) 213–219.
[25] H.Y. Fu, S.R. Zhang, X.H. Wang, T. Saheki, K. Kobayashi, J.S. Wang, The mutation spectrum of the SLC25A13 gene in Chinese infants with intrahepatic cholestasis and aminoacidemia, J. Gastroenterol. 46 (2011) 510–518.
[26] K. Kobayashi, Y.B. Lu, M.X. Li, I. Nishi, K.-J. Hsiao, K. Choeh, Y. Yang, W.-L. Hwu, J.K.V. Reichardt, F. Palmieri, Y. Okano, T. Saheki, Screening of nine SLC25A13 mutations: their frequency in patients with citrin deficiency and high carrier rates in Asian populations, Mol. Genet. Metab. 80 (2003) 356–359.
[27] T. Saheki, K. Kobayashi, M. Iijima, M. Horiuchi, L. Begum, M.A. Jalil, M.X. Li, Y.B. Lu, M. Ushikai, A. Tabata, M. Moriyama, K.-J. Hsiao, Y. Yang, Adult-onset type II citrullinemia and idiopathic neonatal hepatitis caused by citrin deficiency: involvement of the aspartate glutamate carrier for urea synthesis and maintenance of the urea cycle, Mol. Genet. Metab. 81 (Suppl 1) (2004) S20–S26.
[28] J.T. Lin, K.J. Hsiao, C.Y. Chen, C.C. Wu, S.J. Lin, Y.Y. Chou, S.C. Shiesh, High resolution melting analysis for the detection of SLC25A13 gene mutations in Taiwan, Clin. Chim. Acta 412 (2011) 460–465.
[29] Y. Shigematsu, S. Hirano, I. Hata, Y. Tanaka, M. Sudo, N. Sakura, T. Tajima, S. Yamaguchi, Newborn mass screening and selective screening using electrospray tandem mass spectrometry in Japan, J. Chromatogr. B Analyt. Technol. Biomed. Life Sci. 776 (2002) 39–48.
[30] M. Yazaki, Y.-i. Takei, K. Kobayashi, T. Saheki, S.-I. Ikeda, Risk of worsened encephalopathy after intravenous glycerol therapy in patients with adult-onset type II citrullinemia (CTLN2), Intern. Med. 44 (2005) 188–195.
[31] H. Takahashi, T. Kagawa, K. Kobayashi, H. Hirabayashi, M. Yui, L. Begum, T. Mine, S. Takagi, T. Saheki, Y. Shinohara, A case of adult-onset type II citrullinemia—deterioration of clinical course after infusion of hyperosmotic and high sugar solutions, Med. Sci. Monit. 12 (2006) CS13–CS15.

J Gastroenterol (2012) 47:1267–1274
DOI 10.1007/s00535-012-0590-3

ORIGINAL ARTICLE—LIVER, PANCREAS, AND BILIARY TRACT

Do genetic variants in the *SPINK1* gene affect the level of serum PSTI?

Kiyoshi Kume · Atsushi Masamune · Hiroyuki Ariga · Shintaro Hayashi · Tetsuya Takikawa · Shin Miura · Noriaki Suzuki · Kazuhiro Kikuta · Shin Hamada · Morihisa Hirota · Atsushi Kanno · Tooru Shimosegawa

Received: 13 November 2011 / Accepted: 22 March 2012 / Published online: 20 April 2012

Abstract
Background The serine protease inhibitor Kazal type 1 (SPINK1), also known as pancreatic secretory trypsin inhibitor (PSTI), is a peptide secreted by pancreatic acinar cells. Genetic studies have shown an association between *SPINK1* gene variants and chronic pancreatitis or recurrent acute pancreatitis. The aim of this study was to clarify whether the *SPINK1* variants affect the level of serum PSTI.
Methods One hundred sixty-three patients with chronic pancreatitis or recurrent acute pancreatitis and 73 healthy controls were recruited. Serum PSTI concentrations were determined with a commercial radioimmunoassay kit.
Results Ten patients with the p.N34S variant, 7 with the IVS3+2T>C variant, two with both the p.N34S and the IVS3+2T>C variants, and one with the novel missense p.P45S variant in the *SPINK1* gene were identified. The serum PSTI level in patients with no *SPINK1* variants was 14.3 ± 9.6 ng/ml (mean ± SD), and that in healthy controls was 10.7 ± 2.2 ng/ml. The PSTI level in patients carrying the IVS3+2T>C variant (5.1 ± 3.4 ng/ml), but not in those with the p.N34S variant (8.9 ± 3.5 ng/ml), was significantly lower than that in the patients without the *SPINK1* variants and the healthy controls. The serum PSTI level in the patient with the p.P45S variant was 4.9 ng/ml. Low levels of serum PSTI (<6.0 ng/ml) showed sensitivity of 80 %, specificity of 97 %, and accuracy of 96 % in the differentiation of IVS3+2T>C and p.P45S carriers from non-carriers.
Conclusion Serum PSTI levels were decreased in patients with the IVS3+2T>C and p.P45S variants of the *SPINK1* gene.

Keywords Pancreatitis · Serine protease inhibitor Kazal type 1 · Pancreatic secretory trypsin inhibitor · Polymorphism · Mutation

Abbreviations

BMI	Body mass index
CP	Chronic pancreatitis
RAP	Recurrent acute pancreatitis
SPINK1	Serine protease inhibitor Kazal type 1
PSTI	Pancreatic secretory trypsin inhibitor
ROC	Receiver operating characteristic
SD	Standard deviation

Introduction

Chronic pancreatitis (CP) is a progressive inflammatory disease that eventually leads to impairment of the exocrine and endocrine functions of the organ [1, 2]. It has been suggested that pancreatitis results from an imbalance of proteases and their inhibitors within the pancreatic parenchyma, and recent human genetic studies have supported this concept. Gain-of-function mutations in the cationic trypsinogen (protease, serine, 1; *PRSS1*) gene are causes of hereditary pancreatitis [3, 4]. Mutations in the serine protease inhibitor Kazal type 1 (*SPINK1*) gene are thought to diminish protection against prematurely activated trypsin,

K. Kume · A. Masamune (✉) · H. Ariga · S. Hayashi · T. Takikawa · S. Miura · N. Suzuki · K. Kikuta · S. Hamada · M. Hirota · A. Kanno · T. Shimosegawa
Division of Gastroenterology,
Tohoku University Graduate School of Medicine,
1-1 Seiryo-cho, Aoba-ku, Sendai 980-8574, Japan
e-mail: amasamune@med.tohoku.ac.jp

and are thereby linked to trypsin-related pancreatic injury [5–9]. Loss-of-function alterations in the chymotrypsin C (*CTRC*) gene, whose product specifically degrades all human trypsin/trypsinogen isoforms, predispose to pancreatitis by diminishing the protective trypsin-degrading activity of this gene [10]. Of these genes, *SPINK1*, also known as pancreatic secretory trypsin inhibitor (PSTI), provides the first line of defense against premature trypsinogen activation within the pancreas [11]. Previous studies have shown that variants in the *SPINK1* gene are associated with CP of various etiologies including idiopathic, familial, and tropical [5–9, 12]. The p.N34S (c.101A>G) variant has been found worldwide in CP patients and healthy controls, with an average allele frequency of 9.7 and 1 %, respectively [6–9, 13]. We and others have reported that the p.N34S variant is strongly associated with recurrent acute pancreatitis (RAP), but does not increase the risk of the first or sentinel acute pancreatitis event [14, 15]. The second most common haplotype contains the c.-215G>A promoter polymorphism and the IVS3+2T>C (c.194+2T>C) variant which affects the 5′ splicing site in intron 3. This haplotype has been reported in patients with idiopathic, familial, and alcoholic CP [6–8, 16]. Currently, approximately 40 variants in the *SPINK1* gene have been reported (http://www.uni-leipzig.de/pancreasmutation).

The serum levels of PSTI increase in association with severe inflammation, tissue destruction, and malignant diseases, including pancreatitis and pancreatic cancer [17–19 and references therein]. On the other hand, decreased levels of serum PSTI have also been reported [20, 21]. Nakano et al. [20] have shown that serum PSTI was decreased in 2 of 26 patients with calcifying CP, but the level was not decreased in any patients with other digestive diseases. Satake et al. [21] found decreased serum PSTI levels (<5.8 ng/ml) in 4 of 23 patients with CP and in 6 of 30 with pancreatic cancer. But the pathophysiological significance of lower PSTI levels has not been fully determined. We previously examined the mRNA sequences of the *SPINK1* gene and revealed that the IVS3+2T>C variant caused skipping of the whole of exon 3 [22]. Other functional studies have revealed that several missense variants, such as p.G48E, p.D50E, p.Y54H, p.R65Q, and p.R67C, reduce PSTI secretion by causing intracellular retention and degradation [23, 24]. Accordingly, we hypothesized that the serum PSTI levels would be decreased in patients carrying these *SPINK1* variants. The aim of this study was to clarify whether the *SPINK1* variants affected the level of serum PSTI.

Methods

Subjects

All enrolled subjects gave their informed consent according to the ethical guidelines of the Declaration of Helsinki. This study was approved by the Ethics Committee of Tohoku University School of Medicine (article number: 2010-45 and 2010-355; principal investigator: A. Masamune). A total of 114 patients with CP, 49 patients with RAP, and 73 healthy controls were enrolled in this study. The characteristics of the patients are shown in Table 1. None of the patients or control subjects had developed malignant diseases. We recruited relatively young healthy controls (36.6 ± 9.4 years old).

The diagnosis of CP was based on clinical examinations, laboratory tests, radiological findings of pancreatic calcifications by computed tomography and endoscopic ultrasonography, and/or pathological findings such as pancreatic ductal irregularities and dilatations on endoscopic retrograde cholangiopancreatography [2]. The diagnosis of hereditary pancreatitis was made on the basis of three or more relatives in two or more generations with

Table 1 Characteristics of the study population

Etiology	Number of patients			Gender	Age (years)[a]
	CP	RAP	Total	Male:female	
Hereditary	5	0	5	3:2	25.2 ± 16.9
Familial	11	0	11	5:6	27.3 ± 19.6
Idiopathic	28	37	65	33:32	48.3 ± 21.1
Alcoholic	41	10	51	49:2	56.1 ± 12.8
Autoimmune	29	0	29	27:2	58.1 ± 17.0
Divisum	0	2	2	2:0	53.5 ± 2.1
Total	114	49	163	119:44	50.7 ± 19.4
Healthy controls			73	41.32	36.6 ± 9.4

CP chronic pancreatitis, *RAP* recurrent acute pancreatitis

[a] Mean ± SD

CP and/or the confirmation of *PRSS1* gene mutations. Patients in whom the criteria for hereditary pancreatitis were not met but who had at least 2 affected family members were classified as having familial pancreatitis. Idiopathic CP included patients in whom no predisposing factor was identified. Patients with alcohol consumption of more than 80 g/day for at least 2 years were classified as having alcoholic CP. Autoimmune pancreatitis was diagnosed in patients with characteristic findings such as increased levels of serum γ-globulin or IgG_4, the presence of autoantibodies, diffuse enlargement of the pancreas, and diffusely irregular narrowing of the main pancreatic duct. The diagnosis of acute pancreatitis was based on typical clinical features, elevated serum amylase and lipase (three times the upper limit of normal), and positive findings on computed tomography.

Mutational analysis

Genomic DNA was extracted from peripheral blood leucocytes according to the standard protocol. All exons and the promoter region of the *SPINK1* gene were amplified by polymerase chain reaction and directly sequenced as previously described [8].

Measurement of serum PSTI

Most of the blood samples were taken in the morning after fasting, although it has been shown that the serum PSTI level was not influenced by the diet and was stable throughout the day [25]. None of the CP patients was in an acute exacerbation of CP and none of the RAP patients was in the active phase of RAP. The Serum PSTI concentrations were determined with a commercial radioimmunoassay kit (Ab Bead PSTI; Eiken Chemical, Tokyo, Japan). According to the manufacturer, the normal range of the assay was 4.6–20.0 ng/ml, and the serum PSTI concentration could be measured accurately in the range of 0.31–3700 ng/ml. The procedure was as follows. Briefly, a 50-μl serum sample was incubated with an anti-PSTI-antibody-coated bead and 200-μl ^{125}I-labeled anti-hPSTI antibody at room temperature for 3 h. The unreacted ^{125}I-labeled anti-hPSTI antibody was removed, and the radioactivity bound to the bead was measured with a gamma scintillation counter. A logit-log representation of the calibration curve was used to calculate the serum PSTI concentration, with the results expressed in ng/ml.

Statistical analysis

The results were expressed as means ± standard deviation (SD). All statistical analyses were performed using SPSS version 17.0 statistical analysis software (SPSS, Chicago, IL, USA). The significance of differences in the PSTI concentrations was tested by Tukey's honest significance difference test, and that in ages was tested by Student's *t*-test. In addition, we performed a stepwise multiple linear regression analysis to explore the variables independently correlated with the serum PSTI levels. The variables included age, gender, body mass index (BMI), smoking, diagnosis, etiology, and the *SPINK1* variants. Also, the serum PSTI concentration data were dichotomized according to the results of receiver operating characteristic (ROC) curve analyses. Differences in the frequency of low serum PSTI levels (<6.0 ng/ml) between carriers of the IVS3+2T>C and p.P45S variants and non-carriers were analyzed with the two-sided Fisher's exact test. Additional odds ratios with 95 % confidence intervals were calculated. A P value of <0.05 was considered statistically significant.

Table 2 Characteristics of the patients carrying the serine protease inhibitor Kazal type 1 (*SPINK1*) variants

SPINK1 variants	Gender	Age (years)[a]	Diagnosis		Etiology					Total
	Male:female		CP	RAP	Hereditary	Familial	Idiopathic	Alcoholic	Others	
p.N34S	3:7	28.9 ± 16.1	8 (1)	2 (0)	1 (0)	5 (0)	3 (1)	1 (0)	0	10 (1)
IVS3+2T>C	4:3	28.0 ± 25.0	6 (1)	1 (0)	1 (0)	2 (0)	3 (1)	1 (0)	0	7 (1)
IVS3+2T>C/p.N34S[b]	1:1	26.5 ± 16.3	1 (0)	1 (0)	0	0	2 (0)	0	0	2 (0)
p.P45S	0:1	31	1 (0)	0	0	0	1 (0)	0	0	1 (0)
None	111:32	53.6 ± 17.7	98	45	3	4	56	49	31	143
Total	119:44	50.7 ± 19.4	114	49	5	11	65	51	31	163

The numbers of subjects carrying the variants in a homozygous form are shown in parentheses

None of the 73 healthy controls had these *SPINK1* variants

CP chronic pancreatitis, *RAP* recurrent acute pancreatitis

[a] Mean ± SD

[b] Two patients were compound heterozygotes carrying both the p.N34S and IVS3+2T>C variants

Results

Among the 163 patients with CP or RAP, 20 had genetic variants in the *SPINK1* gene. Ten patients had the p.N34S variant (9 heterozygotes and 1 homozygote), 7 had the IVS3+2T>C variant (6 heterozygotes and 1 homozygote), and 2 were compound heterozygotes for the p.N34S and IVS3+2T>C variants (Table 2). As well, a 31-year-old female patient with idiopathic CP had a novel missense variant p.P45S (c.133C>T) in a heterozygous form. She had suffered from multiple attacks of acute pancreatitis since she was 15 years old. She had no family history of pancreatitis. Computed tomography and endoscopic retrograde cholangiopancreatography revealed irregular dilatation of the main pancreatic duct with multiple intraductal pancreatic stones throughout the whole pancreas. None of the 73 healthy controls had *SPINK1* variants.

The serum PSTI levels in the patients and healthy controls are shown in Table 3. The serum PSTI levels in all patients with CP or RAP did not differ from those in healthy controls. The serum PSTI levels did not differ between patients with CP and those with RAP, or between males and females. The IVS3+2T>C variant and BMI were independently correlated with the serum PSTI levels ($P = 0.001$ and $P = 0.02$, respectively). In 42 patients for whom information of the age of onset was available, we examined the correlation between serum PSTI levels and duration of the disease. But no significant correlation was observed ($P = 0.24$). In the 16 patients with hereditary or familial pancreatitis, the serum PSTI levels (8.3 ± 3.1 ng/ml) were lower than those in the other 147 patients with pancreatitis (13.9 ± 9.7; $P = 0.023$). Of note, the 16 patients with hereditary or familial pancreatitis were younger (26.6 ± 18.1 years) than the patients with other etiologies (53.1 ± 18.0 years; $P < 0.001$). In the 10 patients carrying the p.N34S variant, the serum PSTI level was 8.9 ± 3.5 ng/ml, which did not significantly differ from the level in the patients carrying no *SPINK1* variants ($P = 0.17$). The ten patients carrying the p.N34S variant were younger than those with no *SPINK1* variants ($P < 0.001$). The serum PSTI level in the patient with homozygous p.N34S was 6.0 ng/ml. In the 9 patients carrying the IVS3+2T>C variant, including two patients carrying both the p.N34S and IVS3+2T>C variants, the serum PSTI level was lower than that in patients without the *SPINK1* variant ($P < 0.001$) (Fig. 1). The nine patients carrying the IVS3+2T>C variant were younger than those with no *SPINK1* variants ($P < 0.001$). The PSTI level in patients carrying the heterozygous IVS3+2T>C variant was 5.5 ± 3.2 ng/ml, whereas the level in the patient with homozygous IVS3+2T>C was 1.2 ng/ml. The PSTI levels in the two patients carrying both the p.N34S and IVS3+2T>C variants were 3.5 and 3.7 ng/ml. As described below in the 'Discussion', the serum PSTI level increased steadily with advancing age [25]. To clarify whether the decreased PSTI levels in patients carrying the IVS3+2T>C variant merely resulted from differences in ages, we recruited relatively young healthy controls (36.6 ± 9.4 years old) and measured their serum PSTI levels. The serum PSTI levels in patients carrying the IVS3+2T>C variant were lower than those in the healthy controls ($P < 0.001$). The serum PSTI level in the patient carrying the novel missense p.P45S variant was 4.9 ng/ml.

To determine a cut-off value for the serum PSTI level as a predictor of the IVS3+2T>C and p.P45S variants, we performed ROC analysis. A value of 6.0 ng/ml for serum PSTI was taken as the best cut-off value to differentiate IVS3+2T>C and p.P45S carriers from non-carriers and the healthy controls (Fig. 2). According to this cut-off level, the frequency (8/10; 80 %) of a low serum PSTI level in IVS3+2T>C and p.P45S carriers was significantly higher than that (5/153; 3.3 %) in non-carriers ($P < 0.01$, odds ratio 118.4, 95 % confidence interval 19.8–707.7). Low levels of serum PSTI (<6.0 ng/ml) showed a sensitivity of 80 %, specificity of 97 %, and accuracy of 96 % in the differentiation of IVS3+2T>C and p.P45S carriers from non-carriers.

Discussion

The major findings of this study are as follows: (1) identification of a novel missense variant p.P45S in the *SPINK1* gene, (2) the serum PSTI level was decreased in patients with CP or RAP carrying the IVS3+2T>C variant, but not in those carrying the p.N34S variant, (3) the serum PSTI level was not decreased in healthy carriers of the IVS3+2T>C variant, and (4) 6.0 ng/ml was the best cut-off value for serum PSTI to differentiate IVS3+2T>C and p.P45S carriers from non-carriers. Our results suggest that decreased PSTI expression might be the mechanism underlying the susceptibility to pancreatitis in patients carrying the IVS3+2T>C variant. In addition, if the serum PSTI level is low in patients with pancreatitis, the patients might have loss-of-function *SPINK1* variants. In a previous large study employing 797 healthy controls, the normal range of the serum PSTI level, which took the lower and upper limits as 2SDs below and above the control mean, was 5.9–22.7 ng/ml, with a mean of 10.6 ng/ml [25]. Our result that set the lower limit at 6.0 ng/ml was compatible with this large study. Although the genetic diagnosis of patients with pancreatitis is not routinely performed in Japan, measurement of the serum PSTI might be useful to identify patients carrying the loss-of-function *SPINK1* variants.

We have previously shown that the IVS3+2T>C variant caused skipping of the whole exon 3, resulting in the loss of

Table 3 Serum pancreatic secretory trypsin inhibitor (PSTI) levels in the study population

	n	Age (years)	PSTI (ng/ml)	Range	*P* value
Patients (total)	163	50.7 ± 19.4	13.4 ± 9.4	1.2–64.0	–
Gender					
Male	119	52.6 ± 19.1	13.6 ± 8.7	1.2–53.0	0.47
Female	44	45.7 ± 19.6	12.9 ± 11.1	2.8–64.0	
BMI					
≥25	14	56.8 ± 17.6	10.1 ± 2.3	6.6–14.0	0.02
<25	149	50.2 ± 19.6	13.7 ± 9.7	1.2–64.0	
Smoking					
Smoker	82	56.7 ± 13.1	13.5 ± 7.8	3.5–42.0	0.11
Non-smoker	81	44.5 ± 22.8	13.2 ± 10.8	1.2–64.0	
Diagnosis					
CP	114	51.1 ± 19.0	13.7 ± 9.9	1.2–64.0	0.73
RAP	49	49.8 ± 20.5	12.6 ± 8.1	3.5–43.0	
Etiology					
Hereditary	5	25.2 ± 16.9	7.6 ± 1.6	5.9–10.0	0.64
Familial	11	27.3 ± 19.6	8.7 ± 3.6	2.8–18.0	0.63
Idiopathic	65	48.3 ± 21.1	13.0 ± 11.1	1.2–64.0	0.47
Alcoholic	51	56.1 ± 12.8	15.1 ± 9.3	5.9–42.0	0.93
Autoimmune	29	58.1 ± 17.0	14.0 ± 7.0	5.8–32.0	0.82
Divisum	2	53.5 ± 2.1	12.3 ± 6.6	7.6–17.0	0.59
SPINK1					
p.N34S	10	28.9 ± 16.1	8.9 ± 3.5	6.0–18.0	0.25
IVS3+2T>C/p.N34S	2	26.5 ± 16.3	3.6 ± 0.1	3.5–3.7	–
All IVS3+2T>C[a]	9	27.6 ± 22.1	5.1 ± 3.4	1.2–11.0	0.001
p.P45S	1	31	4.9	4.9	–
None	143	53.6 ± 17.7	14.3 ± 9.6	4.7–64.0	0.25
Healthy controls (total)	73	36.6 ± 9.4	10.7 ± 2.2	5.4–17.0	–
Gender					
Male	41	37.4 ± 7.8	10.5 ± 2.4	5.4–17.0	0.55
Female	32	35.5 ± 11.2	10.8 ± 2.0	6.7–15.0	
BMI					
≥25	13	36.9 ± 8.2	10.3 ± 2.6	6.0–16.0	0.07
<25	60	36.5 ± 9.7	10.7 ± 2.1	5.4–17.0	
Smoking					
Smoker	10	37.0 ± 9.1	11.6 ± 2.5	8.2–17.0	0.17
Non-smoker	63	36.5 ± 9.5	10.5 ± 2.2	5.4–16.0	

n number of patients, *CP* chronic pancreatitis, *RAP* recurrent acute pancreatitis, *BMI* body mass index

[a] Includes two patients who were compound heterozygotes carrying both the p.N34S and IVS3+2T>C variants

the trypsin binding site [22]. Functional studies utilizing a minigene system showed that this variant abolished SPINK1 expression at the mRNA level, with consequent loss of inhibitor secretion [13]. Therefore, we supposed that the expression of functionally normal PSTI could be restricted in patients carrying this variant. In the present study, the mean serum PSTI levels in patients with the homozygous and heterozygous IVS3+2T>C variant were 1.2 and 5.7 ng/ml, respectively. It is unclear whether there exists a correlation between the serum PSTI level and that in the pancreatic acinar cells of a given subject. However, our results showing decreased serum PSTI levels in patients carrying this variant agree with previous functional studies and support the concept that, in patients with pancreatitis, the IVS3+2T>C variant decreases PSTI expression not only in the pancreas but also systemically. Interestingly, we found that the serum PSTI level was not significantly decreased in healthy carriers of this variant. Of the five healthy subjects carrying this variant, who were mainly family members of CP patients harboring this

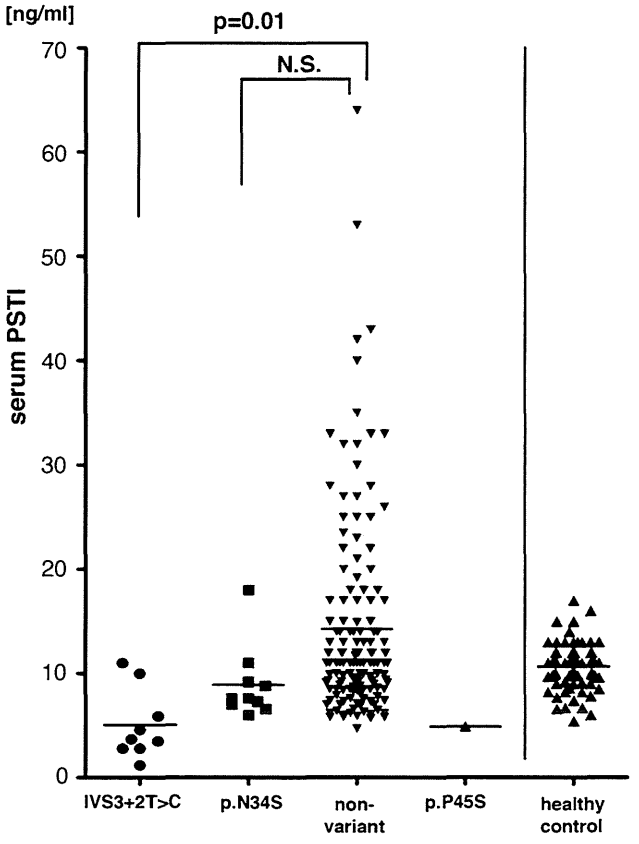

Fig. 1 Serum pancreatic secretory trypsin inhibitor (*PSTI*) levels in patients carrying the serine protease inhibitor Kazal type 1 (*SPINK1*) variants. The distribution of the serum PSTI levels in patients with chronic pancreatitis (CP) or recurrent acute pancreatitis (RAP) is shown. Patients were classified based on the presence or absence of the *SPINK1* variants. Patients with the IVS3+2T>C variants included those carrying both the IVS3+2T>C and p.N34S variants. The *horizontal bars* denote the mean value of each group. *N.S.* not significant

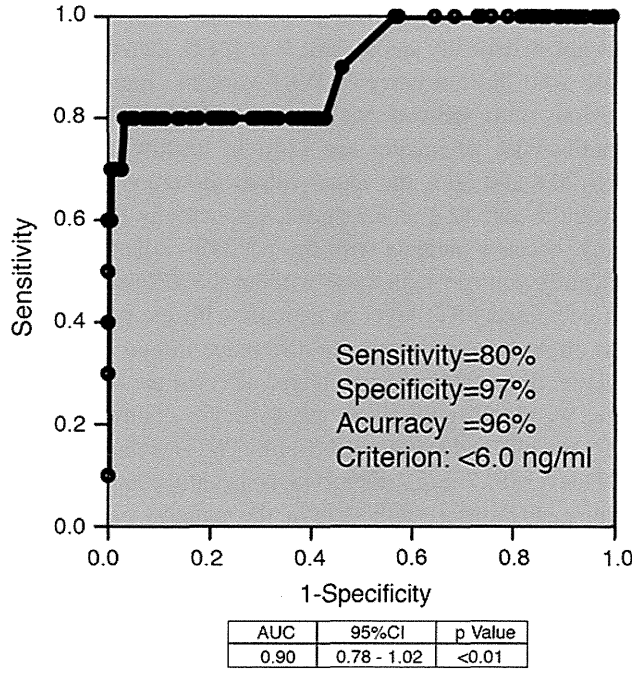

Fig. 2 Receiver operating characteristic (ROC) curve for serum PSTI concentration. The value of 6.0 ng/ml for serum PSTI was taken as the best cut-off to differentiate IVS3+2T>C and p.P45S carriers from non-carriers in patients with pancreatitis. Low levels of serum PSTI (<6.0 ng/ml) showed a sensitivity of 80 %, specificity of 97 %, and accuracy of 96 % in the differentiation of IVS3+2T>C and p.P45S carriers from non-carriers. *AUC* area under the curve, *CI* confidence interval

variant, only one subject had a decreased serum PSTI level (3.6 ng/ml). In the other four healthy subjects carrying this variant, the serum PSTI level ranged between 6.3 and 14.0 ng/ml, and was not decreased. The maintenance of normal PSTI expression by the non-mutated allele might be a mechanism that protects the carriers from developing pancreatitis.

The serum PSTI level was low (4.9 ng/ml) in our one patient with idiopathic CP carrying the novel missense variant p.P45S. None of the 265 healthy subjects carried this variant (A. Masamune, unpublished observation). Although the functional consequence of this variant remains unknown, the decreased level of serum PSTI might reflect reduced PSTI secretion. Indeed, functional studies using human embryonic kidney 293T cells and Chinese hamster ovarian cells showed that several missense variants, such as p.G48E, p.D50E, p.Y54H, p.R65Q, and p.R67C, reduced PSTI secretion by causing intracellular retention and degradation [23, 24]. In addition, Boulling et al. [26] reported that five additional rare missense variants: p.N64D, p.K66N, p.R67H, p.T69I, and p.C79F, caused a complete loss of PSTI expression.

The p.N34S variant is the most common pancreatitis-associated variant in the *SPINK1* gene worldwide [5–9], but the disease-relevant functional effects of the p.N34S variant on SPINK1 structure and function remain obscure. Functional analyses comparing recombinant p.N34S and wild-type SPINK1 found no difference in SPINK1 expression, trypsin inhibitory activity, or binding to trypsin [23, 24, 27]. The aberrant splicing caused by the cosegregating intronic mutations (c.56-37T>C, c.87+268A>G, c.195-606G>A, and c.195-66_65insTTTT) might play a role in the pathogenesis, but reverse transcription-polymerase chain reaction (PCR) analysis of total RNA isolated from surgically resected pancreatic tissues of p.N34S homozygotes failed to reveal aberrant splicing of the *SPINK1* transcript [28]. In addition, Kereszturi et al. [13] showed that all four intronic variants in linkage disequilibrium with the p.N34S variant were functionally harmless. These studies suggest that SPINK1 expression is not altered in patients carrying the p.N34S variant. In the present study, the serum PSTI level in patients carrying the

p.N34S variant tended to be lower (although the difference was not statistically significant; $P = 0.17$), than the level in those who did not carry *SPINK1* variants. Importantly, a previous study showed that the serum PSTI level increased steadily with advancing age [25]. In healthy subjects in their 20 s and 50 s, the mean values of serum PSTI were 9.6 ± 2.6 and 12.2 ± 4.2 ng/ml, respectively [25]. In our study, because patients with the p.N34S variant were significantly younger than those without the *SPINK1* variants, the decreased PSTI level in patients with the p.N34S variant might have reflected the difference in age. To clarify whether the p.N34S variant indeed affected the serum PSTI level, we recruited relatively young healthy controls (36.7 ± 9.4 years old) and measured the serum PSTI levels. The serum PSTI level (10.7 ± 2.2 ng/ml) in the healthy controls did not significantly differ from that in the patients carrying the p.N34S variant, suggesting that the p.N34S variant by itself did not affect the serum PSTI level.

In addition to being increased in patients with pancreatitis and pancreatic cancer, serum PSTI levels have also been shown to be increased in patients with extrapancreatic malignancies such as cholangiocarcinoma [29] and cancers of the colon, breast, and prostate [30, 31]. Based on these findings, PSTI is now also known as a tumor-associated trypsin inhibitor that correlates with disease progression and poor prognosis [19]. High expression of PSTI in cancers may be related to its role in cell proliferation and migration, at least through the activation of the epidermal growth factor receptor/mitogen-activated protein kinase cascade [32]. There are structural similarities between SPINK1 and epidermal growth factor in terms of amino acid residues and the presence of 3 intrachain disulfide bridges. Hence, SPINK1 may bind to epidermal growth factor receptor to activate its downstream signaling pathways. It would be of interest to determine whether mutated SPINK1 affects the serum PSTI levels in cancer and also whether mutated SPINK1 affects the cell behaviors of various cancer cells.

Acknowledgments This study was supported in part by a Grant-in-Aid from the Japan Society for the Promotion of Science (to K. Kume, to A. Masamune, and to T. Shimosegawa), and by the Research Committee of Intractable Pancreatic Diseases (Principal investigator: T. Shimosegawa), provided with funding by the Ministry of Health, Labour, and Welfare of Japan.

Conflict of interest The authors declare that they have no conflict of interest.

References

1. Steer ML, Waxman I, Freedman S. Chronic pancreatitis. N Engl J Med. 1995;332:1482–90.
2. Etemad B, Whitcomb DC. Chronic pancreatitis: diagnosis, classification, and new genetic developments. Gastroenterology. 2001;120:682–707.
3. Whitcomb DC, Gorry MC, Preston RA, Furey W, Sossenheimer MJ, Ulrich CD, et al. Hereditary pancreatitis is caused by a mutation in the cationic trypsinogen gene. Nat Genet. 1996;14:141–5.
4. Masson E, Le Maréchal C, Delcenserie R, Chen JM, Férec C. Hereditary pancreatitis caused by a double gain-of-function trypsinogen mutation. Hum Genet. 2008;123:521–9.
5. Witt H, Luck W, Hennies HC, Classen M, Kage A, Lass U, et al. Mutations in the gene encoding the serine protease inhibitor, Kazal type 1 are associated with chronic pancreatitis. Nat Genet. 2000;25:213–6.
6. Pfützer RH, Barmada MM, Brunskill AP, Finch R, Hart PS, Neoptolemos J, et al. SPINK1/PSTI polymorphisms act as disease modifiers in familial and idiopathic chronic pancreatitis. Gastroenterology. 2000;119:615–23.
7. Chen JM, Mercier B, Audrezet MP, Raguenes O, Quere I, Ferec C. Mutations of the pancreatic secretory trypsin inhibitor (PSTI) gene in idiopathic chronic pancreatitis. Gastroenterology. 2001;120:1061–4.
8. Kume K, Masamune A, Mizutamari H, Kaneko K, Kikuta K, Satoh M, et al. Mutations in the serine protease inhibitor Kazal type 1 (SPINK1) gene in Japanese patients with pancreatitis. Pancreatology. 2005;5:354–60.
9. Aoun E, Chang CC, Greer JB, Papachristou GI, Barmada MM, Whitcomb DC. Pathways to injury in chronic pancreatitis: decoding the role of the high-risk SPINK1 N34S haplotype using meta-analysis. PLoS ONE. 2008;3:e2003.
10. Rosendahl J, Witt H, Szmola R, Bhatia E, Ozsvári B, Landt O, et al. Chymotrypsin C (CTRC) variants that diminish activity or secretion are associated with chronic pancreatitis. Nat Genet. 2008;40:78–82.
11. Rinderknecht H. Activation of pancreatic zymogens. Normal activation, premature intrapancreatic activation, protective mechanisms against inappropriate activation. Dig Dis Sci. 1986;31:314–21.
12. Bhatia E, Choudhuri G, Sikora SS, Landt O, Kage A, Becker M, et al. Tropical calcific pancreatitis: strong association with SPINK1 trypsin inhibitor mutations. Gastroenterology. 2002;123:1020–5.
13. Kereszturi E, Király O, Sahin-Tóth M. Minigene analysis of intronic variants in common SPINK1 haplotypes associated with chronic pancreatitis. Gut. 2009;58:545–9.
14. Aoun E, Muddana V, Papachristou GI, Whitcomb DC. SPINK1 N34S is strongly associated with recurrent acute pancreatitis but is not a risk factor for the first or sentinel acute pancreatitis event. Am J Gastroenterol. 2010;105:446–51.
15. Masamune A, Ariga H, Kume K, Kakuta Y, Satoh K, Satoh A, et al. Genetic background is different between sentinel and recurrent acute pancreatitis. J Gastroenterol Hepatol. 2011;26:974–8.
16. Ota Y, Masamune A, Inui K, Kume K, Shimosegawa T, Kikuyama M. Phenotypic variability of the homozygous IVS3+2T>C mutation in the serine protease inhibitor Kazal type 1 (SPINK1) gene in patients with chronic pancreatitis. Tohoku J Exp Med. 2010;221:197–201.
17. Ogawa M, Kitahara T, Fujimoto K, Tanaka S, Takatsuka Y, Kosaki G. Serum pancreatic secretory trypsin inhibitor in acute pancreatitis. Lancet. 1980;2:205.
18. Lasson A, Borgström A, Ohlsson K. Elevated pancreatic secretory trypsin inhibitor levels during severe inflammatory disease, renal insufficiency, and after various surgical procedures. Scand J Gastroenterol. 1986;21:1275–80.
19. Paju A, Stenman UH. Biochemistry and clinical role of trypsinogens and pancreatic secretory trypsin inhibitor. Crit Rev Clin Lab Sci. 2006;43:103–42.
20. Nakano I, Funakoshi A, Sumii T, Miyazaki K, Oogami Y, Kimura T, et al. Appearance mechanism and molecular

heterogeneity of serum pancreatic secretory trypsin inhibitor (PSTI). Gastroenterol Jpn. 1985;20:354–60.
21. Satake K, Inui A, Sogabe T, Yoshii Y, Nakata B, Tanaka H, et al. The measurement of serum immunoreactive pancreatic secretory trypsin inhibitor in gastrointestinal cancer and pancreatic disease. Int J Pancreatol. 1988;3:323–31.
22. Kume K, Masamune A, Kikuta K, Shimosegawa T. [-215G>A; IVS3+2T>C] mutation in the SPINK1 gene causes exon 3 skipping and loss of the trypsin binding site. Gut. 2006;55:1214.
23. Király O, Wartmann T, Sahin-Tóth M. Missense mutations in pancreatic secretory trypsin inhibitor (SPINK1) cause intracellular retention and degradation. Gut. 2007;56:1433–8.
24. Boulling A, Le Maréchal C, Trouvé P, Raguénès O, Chen JM, Férec C. Functional analysis of pancreatitis-associated missense mutations in the pancreatic secretory trypsin inhibitor (SPINK1) gene. Eur J Hum Genet. 2007;15:936–42.
25. Ogawa M. Normal level and normal range of serum PSTI concentration. In: Kosaki G, Ogawa M, editors. Pancreatic secretory trypsin inhibitor. Tokyo: Igaku Tosho Shuppan; 1985. p. 91–3 (in Japanese).
26. Boulling A, Keiles S, Masson E, Chen JM, Férec C. Functional analysis of eight missense mutations in the SPINK1 gene. Pancreas. 2011;41:329–30.
27. Kuwata K, Hirota M, Shimizu H, Nakae M, Nishihara S, Takimoto A, Mitsushima K, Kikuchi N, Endo K, Inoue M, Ogawa M. Functional analysis of recombinant pancreatic secretory trypsin inhibitor protein with amino-acid substitution. J Gastroenterol. 2002;37:928–34.
28. Masamune A, Kume K, Takagi Y, Kikuta K, Satoh K, Satoh A, Shimosegawa T. N34S mutation in the SPINK1 gene is not associated with alternative splicing. Pancreas. 2007;34:423–8.
29. Tonouchi A, Ohtsuka M, Ito H, Kimura F, Shimizu H, Kato M, Nimura Y, Iwase K, Hiwasa T, Seki N, Takiguchi M, Miyazaki M. Relationship between pancreatic secretory trypsin inhibitor and early recurrence of intrahepatic cholangiocarcinoma following surgical resection. Am J Gastroenterol. 2006;101:1601–10.
30. Gaber A, Johansson M, Stenman UH, Hotakainen K, Pontén F, Glimelius B, Bjartell A, Jirström K, Birgisson H. High expression of tumour-associated trypsin inhibitor correlates with liver metastasis and poor prognosis in colorectal cancer. Br J Cancer. 2009;100:1540–8.
31. Paju A, Hotakainen K, Cao Y, Laurila T, Gadaleanu V, Hemminki A, Stenman UH, Bjartell A. Increased expression of tumor-associated trypsin inhibitor, TATI, in prostate cancer and in androgen-independent 22Rv1 cells. Eur Urol. 2007;52:1670–9.
32. Ozaki N, Ohmuraya M, Hirota M, Ida S, Wang J, Takamori H, Higashiyama S, Baba H, Yamamura K. Serine protease inhibitor Kazal type 1 promotes proliferation of pancreatic cancer cells through the epidermal growth factor receptor. Mol Cancer Res. 2009;7:1572–81.

CLINICAL REPORT

AMERICAN JOURNAL OF medical genetics PART A

Myelodysplastic Syndrome in a Child With 15q24 Deletion Syndrome

Yoko Narumi,[1]* Masaaki Shiohara,[2,3] Keiko Wakui,[1] Asahito Hama,[4] Seiji Kojima,[4] Kentaro Yoshikawa,[2] Yoshiro Amano,[5] Tomoki Kosho,[1] and Yoshimitsu Fukushima[1]

[1]Department of Medical Genetics, Shinshu University School of Medicine, Matsumoto, Japan

[2]Department of Pediatrics, Shinshu University School of Medicine, Matsumoto, Japan

[3]Division of Hematology, Oncology, and Immunology, Nagano Children's Hospital, Azumino, Japan

[4]Department of Pediatrics, Nagoya University Graduate School of Medicine, Nagoya, Japan

[5]Department of Pediatrics, Nagano Red Cross Hospital, Nagano, Japan

Received 10 July 2011; Accepted 24 October 2011

15q24 deletion syndrome is a recently-described chromosomal disorder, characterized by developmental delay, growth deficiency, distinct facial features, digital abnormalities, loose connective tissue, and genital malformations in males. To date, 19 patients have been reported. We report on a 13-year-old boy with this syndrome manifesting childhood myelodysplastic syndrome (MDS). He had characteristic facial features, hypospadias, and mild developmental delay. He showed neutropenia and thrombocytopenia for several years. At age 13 years, bone marrow examination was performed, which showed a sign suggestive of childhood MDS: mild dysplasia in the myeloid, erythroid, and megakaryocytic cell lineages. Array comparative genomic hybridization (array CGH) revealed a de novo 3.4 Mb 15q24.1q24.3 deletion. Although MDS has not been described in patients with the syndrome, a boy was reported to have acute lymphoblastic leukemia (ALL). The development of MDS and hematological malignancy in the syndrome might be caused by the haploinsufficiency of deleted 15q24 segment either alone or in combination with other genetic abnormalities in hematopoietic cells. Further hematological investigation is recommended to be beneficial if physical and hematological examination results are suggestive of hematopoietic disturbance in patients with the syndrome.

Key words: 15q24 deletion syndrome; thrombocytopenia; neutropenia; myelodysplastic syndrome

How to Cite this Article:
Narumi Y, Shiohara M, Wakui K, Hama A, Kojima S, Yoshikawa K, Amano Y, Kosho T, Fukushima Y. 2012. Myelodysplastic syndrome in a child with 15q24 deletion syndrome.
Am J Med Genet Part A 158A:412–416.

INTRODUCTION

Chromosome 15q24 deletion syndrome [OMIM#613406] is a recently-described disorder characterized by developmental delay, growth deficiency, distinct facial features, digital abnormalities, loose connective tissue, and genital malformations in males [Sharp et al., 2007]. Additional features include diaphragmatic hernia, bowel atresia, and congenital heart defects. The syndrome results from the interstitial deletion of the long arm of chromosome 15, typically detected by array comparative genomic hybridization (array CGH). To date, 19 patients with the syndrome have been reported [Smith et al., 2000; Sharp et al., 2007; Klopocki et al., 2008; Marshall et al., 2008; Andrieux et al., 2009; El-Hattab et al., 2010; Masurel-Paulet et al., 2009; Van Esch et al., 2009; El-Hattab et al., 2010; McInnes et al., 2010]. The patients shared some major clinical features.

Although El-Hattab et al. [2009] described a boy with the syndrome showing acute lymphoblastic leukemia (ALL), the relationship between hematological abnormalities and 15q24 deletion syndrome has not been reviewed. Here, we report on a boy with the syndrome manifesting myelodysplastic syndrome (MDS). MDS is a clonal disorder characterized by ineffective hematopoiesis, frequently progress to acute myeloid leukemia [Niemeyer et al., 2005]. We speculate on the mechanism of hematological abnormality in the syndrome.

Grant sponsor: Ministry of Education, Culture, Sports, Science and Technology of Japan; Grant number: 22790972; Grant sponsor: Japanese Ministry of Health, Welfare, and Labor.
*Correspondence to:
Yoko Narumi, M.D., Ph.D., Department of Medical Genetics, Shinshu University School of Medicine, 3-1-1 Asahi, Matsumoto 390-8621, Japan.
E-mail: ynarumi@shinshu-u.ac.jp
Published online 2 December 2011 in Wiley Online Library (wileyonlinelibrary.com).
DOI 10.1002/ajmg.a.34395